
Università Politecnica Delle Marche

Engineering Faculty

Master Degree in Biomedical Engineering

# DEVELOPMENT OF AN ALGORITHM FOR EXTRACTING FOOTBED ANTHROPOMETRIC FEATURES FROM 3D SHOE LAST SCANNING

Advisor:

*Prof.* Marco Mandolini

Co-Advisor:

*Ing.* Paolo Bellelli

Degree Thesis of:

Michele Paris

Academic Year 2020-2021

# I. Summary

# II. List of Figures

# III. List of Table

# 1 Introduction

It is estimated that only about the 20% of the worldwide population have a so-called "perfect feet". For the rest of the population some abnormalities in the foot or ankle structure and functions are present. In the case of serious deformities or dysfunctions of the foot and ankle, the most used non-surgical treatment is represented by the orthopedic footwear and orthosis.

The orthopedic footwear is a special type of shoe designed to accommodate the need of subjects suffering of several foot disorders, medical conditions or diseases. In presence of really severe conditions, custom-made footwear can be realized to better meet the patient's needs.

In this context it is located the company Duna S.r.l.. It is national market leader and one of the major European players in the orthopedic footwear production. The innovation and quality research are the company's cornerstones to offer the best solution to any type of problem, combining grade functional effectiveness and attention to aesthetics.

This thesis work stems from the company's interest to improve and automate the production process of the custom-made footbed. The footbed is the most important structural element of a footwear. It is the component on which both upper and outsole are fixed and therefore it is responsible for the stability, durability and cushioning of the shoe.

During the last decades the development process of the custom-made orthopedic footwear has been characterized by a strong computerization. However, the footbed is still placed in the background because it seems to have a marginal role.

In fact, in the literature and on the market are available many software and tools dedicated to the design and development of customized insoles and lasts, but none on the design of custom-made footbed.

The current footbed design process, proposed by Duna S.r.l., is closely related to the graphic capabilities of the CAD technician who identify the outer edge of the lower surface of a digital scanning last, corresponding to the contour of the element. Since the initial profile curve is designed "manually" by the CAD technician, the current process lacks of accuracy and repeatability.

On the basis of these considerations, the aim of this thesis work is the development of an algorithm for the automatic extraction of the footbed profile curves and other related components starting from a digital last or from a scan of last.

To achieve this goal and thereby overcame the high subjectivity of the actual procedure, a possible solution has been identified in the use of algorithm for the extraction of characteristic curves as a starting point to extract the lateral profile curve of the footbed.

Many methods for the feature line extraction have been proposed in recent decades. Among them, a common strategy is to recognize sharp edges or feature points, and then connect them to form feature curves. However, these methods achieve satisfactory results on noise-free data. To cope with noise, several incremental approach methods have been proposed.

Since the algorithm developed is built to work with meshes obtained by scanning physical lasts, it is obvious a certain presence of noise. For this reason an incremental algorithm is selected. In particular, the algorithm for feature lines extraction implemented inside the procedure for the automatic design of footbed, is the one presented by Hildebrandt et.al in the paper "Smooth Feature Line on Surface Mesh" [1].

The new procedure presented uses the feature lines algorithm to identify the characteristic points of the footbed profile and subsequently, starting from that points, the final footbed, heel reinforcement and benefit sole curves are designed.

The new procedure was validated using a dataset of 162 scans of lasts all belonging to custom-made footwear orders, received by Duna S.r.l.. Among the total dataset, only 90 scans were suitable to be submitted to the algorithm, as they didn't have a sufficient lateral edge for proper analysis.

The 90 meshes were subdivided in two subsets, respectively of 38 (Original) and 52 (Preprocessed) meshes, in order to evaluate the effect of a preprocessing step applied only on the biggest dataset.

The final curves obtained with the new procedure were compared with the curves designed by the CAD technician of Duna S.r.l.. The comparison was made in terms of mean positive and negative deviation and standard deviation between the two curves.

The results obtained show a prevalent footbed profile curves smaller respect to the Duna's footbed curve. However, the variation of the curve of the preprocessed dataset provides an error smaller respect to that shown by the curve variation of the original dataset.

In addiction to the 90 meshes analyzed, 4 additional scans were submitted to the algorithm. Once the final curve were designed, they were also cut at the cutting bench. In this way it was also possible to make a physical comparison with the same physical components designed by Duna S.r.l. and with respect to the physical last.

From this double comparison it emerges that the digital comparison is in line with those of the other 90 cases, while the physical one allows to understand the real impact of this error.

# 2 Industrial - Technical Background

## 2.1 Orthopedic footwear

The word **orthopedic** comes from the Greek "*orthos*", meaning "straight, correct" and "*paideia*", meaning "education". The term was originally used for children and the kind of treatment they received for skeletal deformities, especially regarding the lower locomotor apparatus.

Orthopedic footwear are shoes used to correct, accommodate or prevent a physical deformity or range of motion malfunction in a diseased or injured part of the ankle or foot. This typology of footwear is classified as medical devices.

Nowadays, with the new knowledges acquired in the field of biomechanics and the use of methods assisted by computerized systems, the construction of orthopedic footwear is carried out with technical-scientific rules, which aim, to restore the functionality of the foot taking into account the static, the dynamics, the lower limb, the spine and the aesthetic part [2].

An orthopedic footwear is built from the same elements as a regular shoe, but some of these are processed in order to confer certain characteristics and design features to carry out corrective actions and give greater comfort to the foot.

The most relevant characteristics and design features that identify the orthopedic from the regular shoes are:

- Extra widths and more sizing options.
- Taller upper-soles, for people that need more space for their feet as who suffering from "clawed" or "crossed-over toes".
- Easier to fasten, thanks to a hook-and-loop closure system easier to tighten for subjects living with restricted mobility.
- Seamless upper-soles in order to remove areas that might cause rubbing or abrasion.

- A firm and supportive heel to support the rear of the foot.
- A well cushioned and strong outer-sole and mid-sole, characterized by flex point and impact absorption properties.

There are two typologies of orthopedic footwear available on the market: **mass-produced** orthopedic shoes and **custom-made** orthopedic shoes.

Mass-produced orthopedic footwear is the most frequently used solution for pedorthic patients. It is mainly used by patients with less complex pathologies but who still need the use of an orthopedic shoe. It could be designed to accommodate a custom-made orthosis or an orthopedic insole.

Custom-made orthopedic footwear is typically recommended for the most serious or complex cases. The production starts from row materials to the final product that could also include other pedorthic devices, such as orthotics and braces. This medical device is designed specifically to meet the patient's needs and its manufacture requires an advanced scientific technical knowledge. Hence it is the most complex and costly pedorthic treatment solution.

## 2.2 Custom-made Orthopedic Footwear

Custom - made orthopedic footwear are produced for specific type of patients. Based on the pathology and deformity of the subject and related to the task to be performed, it can be classified from a functional point of view.

The first typology is the **corrective** orthopedic shoe. It is developed for subjects suffering from reversible deformity, which can be led back to normal conformation of the foot. The medical device must maintain a certain physiological and anatomical attitude of the foot, opposing to the forces that cause deformity.

The second one is the orthopedic **support** shoe. It is used in subject suffering from irreversible deformities. The footwear should prevent the deterioration of them and ensures normal walking.

Another typology is the orthopedic shoe for **compensation**. It compensates for the actual or apparent shortening of a limb or replace the missing part of a foot supporting the load and allowing walking.

### *2.2.1 Feet measurement*

The acquisition of both feet measurements is essential to build a comfortable and well designed shoes. It is advisable to carry out the measurements with a resting foot.

The first measurement is the **ball girth**. It is the circumference of the foot in proximity of the distal end of the metatarsals, in other words the circumference before the toes. Then, there is the **behind ball girth** that consists in the circumference measured at the proximal end of the metatarsals. The third measurement concerns the **instep girth**, the front of the foot corresponding to the point where it is articulated with the ankle [3]. Another essential information is the **heel girth** that is the circumference taken between the heel and the instep. The last circumference measured concerns the **ankle girth**.

In addition to this information, the orthopedic technician also takes in consideration the **length of the foot** and the **height of the ankle**, respectively the maximum horizontal distance from the center of the rear heel to the extremity of the protruding finger and the distance from the lower part of the heel to the malleolus.

All these measurements are reported in centimeters (cm) [4] and they are visible on Figure 2.1.

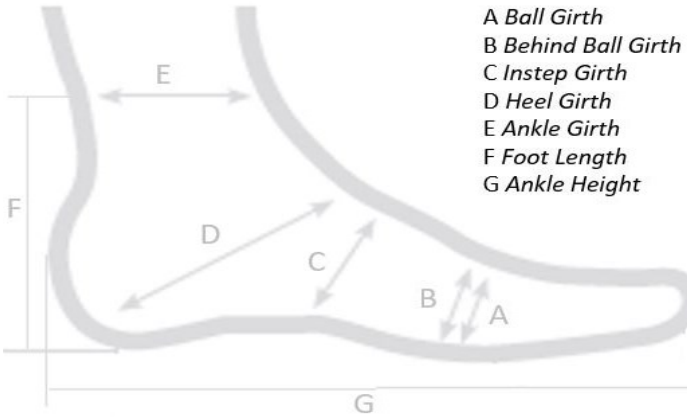


*Figure 2.1: Foot measurements.*

### *2.2.2 Shoe elements*

A custom-made orthopedic footwear is usually composed of six principal components:

- The **upper**. It is the portion of the shoe over the sole and it includes lining, inner cover in leather or fabric, and the closure of the footwear. The external part can be made of different materials ranging from suede leather to various fabrics.
- The **outsole**. It is the bottom element of the shoe, particularly resistant, whose lower surface during the ride is partially or totally in contact with the ground. Usually, it is made of rubber material and may present corrections according to the pathology of the subject. It is the element intended to protect the sole of the foot. It is usually made of vulcanized rubber or synthetic materials with the same properties.
- The **footbed**. It is the element immediately over the outsole and it is an essential building element that allows to assemble the upper and the outsole. In addiction to that, it is responsible for the cushioning, stability and durability of the shoe. It is made in leather, especially in Italy, or synthetic materials such as synthetic material in resin matrix dispersion.
- The **toe cap**. It is located between the upper and the lining in correspondence of the tip and it has the aim to give both the shape to the shoe and above all to protect the foot. It is made with different materials depending on the pathology of the foot.
- The **counter**. It is a rear reinforcement of the shoe located between the upper and the lining in correspondence of the hell. It is used to stiffen the back of the footwear. Originally made of leather, it can now be made of various other materials.
- The **heel reinforcement**. It goes from the area of the heel to the plantar area, getting thinner and thinner. It is essential to keep the sole's heel steady and it is often made with fiberboard, leather or plastic.

A scheme of footwear with the elements already mentioned is visible in Figure 2.2.

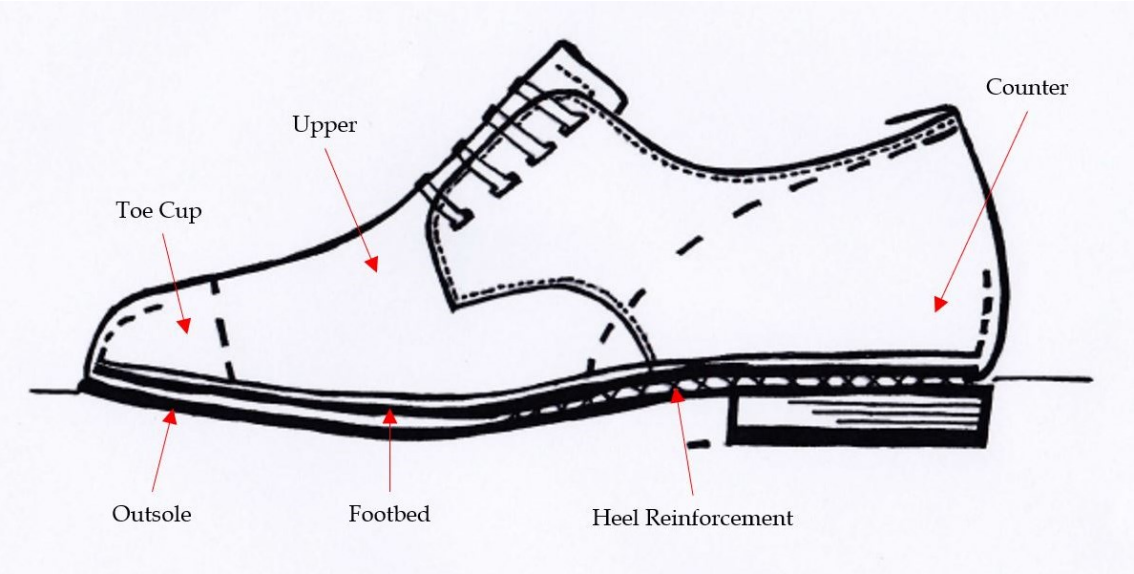


*Figure 2.2: Principal footwear elements.*

These components, if presents, are all firmly part of the shoe and therefore they cannot be removed. In addition to these components, the custom-made orthopedic footwear can be equipped with other three elements:

- **Orthopedic insole**, a mass-produced orthopedic device that consists of a particular type of semi-rigid sole to be inserted in the shoes. It is used to correct the distribution of the body load during the foot support phase and it must be built to avoid foot pain.
- **Orthosis**, a medical device with a role similar to that of orthopedic insole. The main difference between these devices is that the orthosis has a custom-made production related with the pathology, anatomy, age, weight, other anatomical characteristics and information of the single patient. Thus, it is unique.
- **Benefit sole**, an element that can have a variable thickness, ranging from 3 to 10 mm. It has a filling function for certain pathologies and it is especially used when an extra volume of the shoes is required.

It is necessary to consider an additional element that is never present in the final footwear but it is essential for the production of a correct custom-made orthopedic footwear. This element is the "**last**". It is the first component to be made even if in the final product it is not present because it is the basis around which the shoe is built.

A last is a very precise model or mold of the foot and ankle structure built from a casting or three-dimensional digitizing system to produce an accurate representation of the foot. Typically, it is made of wood, Figure 2.3A, or plastic resin, Figure 2.3B, and the construction can take place from a negative chalk or from a measurement module. In this second situation the last is chosen in relation to the model of the shoe and then suitably adapted. Nowadays, in addition to these traditional techniques a last can be designed through dedicated CAD systems starting from a digital acquisition and then turned, or digitally elaborated for the design of some elements.

The last is essentially responsible for the adjustment, the assembly and the fit of the shoe. In case of foot diseases, the last design process is even more important with respect to traditional footwear industry. In fact, the last is the structure on which are defined the corrections and the orthopedic performance of the final product. In this case the last is made of wood, cork and plastic resin together. In particular, starting from a last of a material, layers of other material are added to reach the necessary volume according to the needs of the patient.


*Figure 2.3: Last examples. (A) Shows a last made with wood. (B) Shows a last made with plastic resin.*

### *2.2.3 Building materials*

An orthopedic footwear is made by many different materials. Each element has its own set of materials suitable for its production.

The most commonly used is **leather**, a material obtained from the skin of animals which, following a tanning process, is rendered not putrescible. The leather has characteristics of resistance and especially very high hygiene that make it particularly suitable for the production of many elements. It promotes transpiration and therefore it avoids the development of mold, fungus and other diseases that can afflict the foot due to stagnation of moisture inside the footwear.

The leather has many applications, and it is used mainly for the production of footbed, especially for the Italian market, but also to produce heel reinforcement and benefit sole.

Another material widely used is **plastic** made of expanded polyvinylchloride (PVC). It is particularly suitable for direct printing or laser cutting. It is easily shaped, light but resistant and these features make it ideal for hell reinforcement production.

**Synthetic material in resin matrix dispersion** is a hardness non-woven material with excellent capacity for heat forming. It has good elastic properties and provides a high strength stretch, as well as an easy and high-quality bonding. It is specifically developed for the footbed production of footwear for most of the European market.

**Rubber** is a material characterized by a high elasticity that give them the possibility of being lengthened considerably and being able to quickly return to the initial configuration. Thanks to this feature, it has a good ability to absorb impacts and is therefore used in the production of the outsole.

The last consideration on the materials used to build an orthopedic footwear concerns the production of orthopedic insoles and orthosis. During the last decades many materials were tested in order to achieve the best comfort and wellness for the subject. Nowadays, **Ethylene-vinyl acetate** (EVA) foam is mostly used in orthotic shoe insoles because it helps realize lightweight footwear with high comfort, resiliency, and durability [5]. It is a copolymer plastic of ethylene and vinyl acetate, it is resistant to fungus and bacteria, hypoallergic and non-toxic. For these features, orthosis in EVA foam is widely used in the treatment of foot pain ulcers, which are commonly experienced by diabetic patients.

## 2.3 Foot pathologies

A normal foot is characterized by a specific alignments and joint range of motions measured in a static position. The neutral position of the subtalar joints is a hypothetical reference point from which the clinician can describe and observe variations from the norm and also facilitate anthropometric measurements.

Orthopedic footwear and orthotics are prescribed to treat a range of foot abnormalities e deformities. These malformations can have a strictly musculoskeletal origin or be a secondary consequence of diseases not purely musculoskeletal.

### *2.3.1 Musculoskeletal Deformities*

In the musculoskeletal malformations, the position-based pathology of the foot is considered. One of these is the **rearfoot varus**, a congenital structural abnormality of the rearfoot, where the rearfoot is inverted relative to the weight-bearing surface, when the subtalar joint is in its neutral position and the midtarsal joint is maximally pronated around both axes [6].

It is most commonly a result of a congenital varus abnormality of the leg or foot. Occasionally fractures or other severe trauma can result in a unilateral abnormality. Rearfoot varus is present in a significant portion of population. Considering a rearfoot varus of less than 4°, it is present in 98% of the population. At this level it is not really a pathological condition because the human body has the capability to compensate completely or partially the deformities of the foot applying an additional subtalar joint pronation that is abnormal and excessive but allows the planta aspect of the hell to contact the ground fully, so that ground reaction forces are fairly distributed across the heel.

The worse condition is the uncompensated rearfoot varus when no additional subtalar joint pronation is available for the compensation. The calcaneus remain inverted to the ground during stance and the medial side of the heel does not bear weight effectively [7].

A graphical simulation of the compensated and uncompensated Rearfoot Varus is reported in Figure 2.4.

The treatment of Rearfoot Varus depends on the severity. For the compensated rearfoot varus it has the aim to negate the need for compensatory pronation in the long term. This is achieved by functional foot orthoses with intrinsic or extrinsic medial posting. For what concerns the uncompensated condition, the feet lack mobility and thus require an accommodative orthosis, which offloads and protects, with appropriate bespoke shoe.

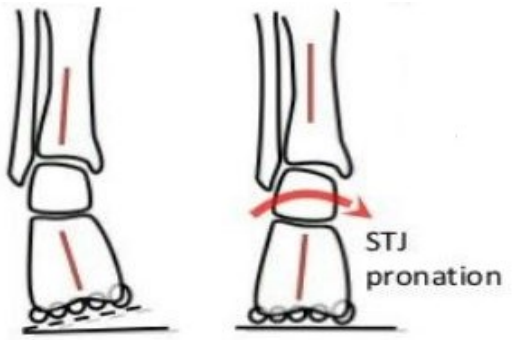


*Figure 2.4: Posterior view of left Rearfoot Varus. On the left the Uncompensated Rearfoot Varus with rear foot inverted and medial side of the heel elevated. On the Right the Compensated Rearfoot Varus with the compensatory STJ pronation.*

In addition to Rearfoot Varus, it exists also the **Forefoot Varus**. It is a congenital osseous structural deformity in which the plantar plane of the forefoot is inverted relative to the plantar plane of the rearfoot when the subtalar joint is in its neutral position and the midtarsal joint is maximally pronated around its axis [8].

The causes of this condition are not well understood but it is assumed to be an inherited structural condition in which there is a reduction in the normal valgus rotation development of the head and neck of the talus. The forefoot varus is classified according to the amount of available compensatory subtalar joint pronation. A fully compensated forefoot varus has a normal contact until the midpoint of midstance. The calcaneum, therefore, becomes everted, as the subtalar joint is abnormally and excessive pronated.

In an uncompensated forefoot varus, which is the most severe condition, the plantar plane of the foot is inverted relative to the plantar plane of the rearfoot and inverted relative to the ground, the calcaneum is vertical, the subtalar joint is in its neutral position and the midtarsal joint is maximally pronated on both its axis. An example of Uncompensated and Compensated Forefoot Varus is shown in Figure 2.5.

The treatment is similar to that of rearfoot varus. In the case of Varus forefoot completely compensated, orthoses to reduce the compensatory excessive pronation of the subtalar joint are prescribed, while with uncompensated deformities bespoke shoes and orthosis to accommodate the abnormality are necessary.

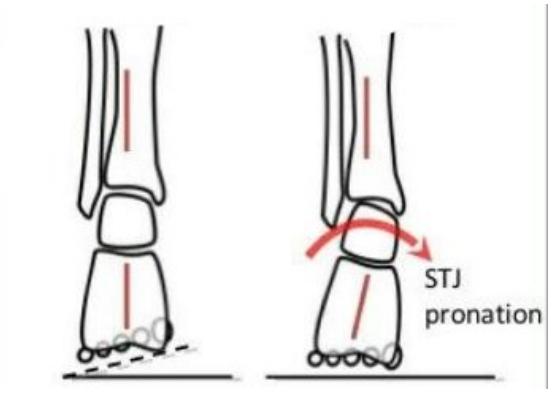


*Figure 2.5: Posterior view of the left Forefoot Varus. On the left the Uncompensated Forefoot Varus. On the right the Compensated Forefoot Varus.*

The **forefoot supination** is an acquired soft-tissue deformity of the longitudinal axis of the midtarsal joint, where the forefoot is inverted relative to the rearfoot when the subtalar joint is in the neutral position and the midtarsal joint is maximally pronated around both its axis. It is a consequence of an excessive pronation at the subtalar joint, where eversion of the calcaneum results in forced compensatory inversion of the forefoot [7].

The treatment consists in the control of abnormal calcaneal eversions using orthosis.

Another pathological condition is the **everted or valgus forefoot**. It is a congenital osseous deformity where the plantar plane of the forefoot is everted relative to the plantar plane of the rearfoot when the subtalar joints is in the neutral position and the midtarsal joint is maximally pronated around both its axes.

It is caused by an excessive amount of developmental valgus rotation resulting in the plantar plane of the forefoot being everted in relation to that of the rearfoot. It is classified as total forefoot valgus if the eversion is complete and the metatarsal heads are all in line one with each other but everted relative to the forefoot; or partial forefoot valgus if the first ray is plantar flexed in relation to the lesser metatarsal heads.

All these conditions can occur singularly on the foot conformation, but in the majority of the cases they are present in a multiple combination inside of the foot pathological posture. The two most frequent foot posture are pes planus and pes cavus.

**Pes planus** describes a foot with a low medial longitudinal arch (MLA), an everted rearfoot and a dorsiflexed and abducted midfoot [9]. Pes planus is often subclassified into rigid and flexible pes planus, as either state causes a different significant effect on foot and limb function, and each requires a different range of management strategies.

The rigid pes planus presents a tarsal coalition or a congenital vertical talus while the flexible one may be asymptomatic or symptomatic with pain and functional limitations. The flexible pes planus affects the 23% of adult population and it provokes alterations of the rearfoot, foot and ankle kinetics, as well as physical function and plantar pressures during gait.

The most useful treatment for flexible pes planus is represented by orthopedic footwear and foot orthosis in order to reduce pain and rearfoot eversion, improve functions and accommodate the high level of deformity for the most severe conditions.

**Pes cavus** describes a foot that has a high MLA, a varus rearfoot, a plantar-flexed first metatarsal and clawing of the digits [10]. It occurs bilaterally in 8-15% of the population with relative foot pain. Pes cavus is classified as idiopathic or neurogenic.

However, in a significant number of cases no clear etiology can be identified and, thus, they are classified as idiopathic. This second classification includes rigid plantar-flexed first ray, rigid forefoot valgus, limb length inequality, where the foot of the shorter leg supinates and pseudo ankle equinus.

In addition to this classification, mobile pes cavus is a term used to describe a foot in which, in the non-weight-bearing state, the medial arch appears excessively high but flattens to a more normal profile when the patient stands.

The treatment of this condition depends on the presenting symptoms, the resultant gait dysfunction and the degree of foot joint mobility. Foot orthosis have been recommended to redistribute plantar pressure, but it is necessary also a proper footwear relating with the height of the midfoot.

Figure 2.6 shows the lower surface of the foot in contact with the ground, the rear and the side view of the foot respectively for a normal, pes cavus and pes planus conformation.

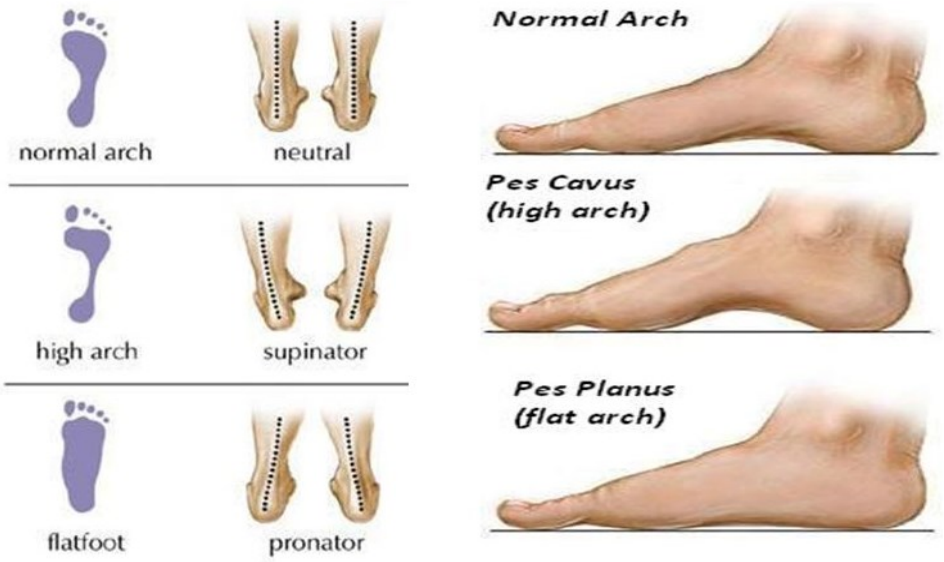


*Figure 2.6: Foot posture. The upper level shows the normal safe conformation. In the middle is shown the Pes Cavus conformation and in the lower level is shown the Pes Planus conformation. For each conformation it is present the lower support, the rear view of the foot and the side view.*

In the musculoskeletal malformations are included also the pathologies of the toe and metatarsophalangeal joints (MTPJ)s. The most recurrent are the Limitus/Rigidus Hallux and the Hallux Valgus.

**Hallux limitus** and **hallux rigidus** describe the progressive structural restriction of the sagittal plane range of motion at the first MTPJ. MTPJ acts as a rocker, facilitating sagittal plane motion and sufficient first MTPJ dorsiflexion enables the body's center of mass to progress forward with a smooth transfer of weight from the loaded to the contralateral foot [11], [12].

Hallux limitus is subdivided into functional and structural. The first presents reduced dorsiflexion of MTPJ only when the foot is weight bearing, the second one in both the weight bearing and the non-weight bearing.

The movement of the hallux in normal and pathological conformation, both limitus and rigidus, are observable in Figure 2.7.

Hallux limitus and Hallux rigidus can be treated conservatively or by surgery. In the conservative treatment is considered also orthopedic footwear. In particular the main features recognizable in this treatment are deep toe box and low heel to reduce forefoot loading, a rigid sole with a half shank to increase shoe stiffness and a rocker sole to reduce the required dorsiflexion of the hallux.

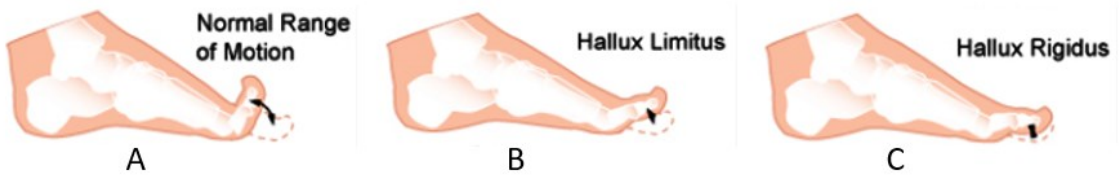


*Figure 2.7: Hallux Limitus/Rigidus. (A) Shows a normal motion. (B) Shows the Hallux Limitus conformation. (C) Shows the Hallux Rigidus conformation.*

**Hallux valgus** is the most recognizable deformity of the foot. it is characterized by a lateral deviation of the great toe and medial deviation of the first metatarsal [13].

It is a complex, progressive and permanent triplane foot deformity, with the formation of exostosis and bursa at the medial aspect of the head of the first metatarsal. The causes of the hallux valgus are manifold. They can be identified in occupation, genetic predisposition, muscle imbalances, anatomical variations, pes planus and ill-fitting footwear.

An example of Moderate Hallux Valgus and Severe Hallux Valgus are shown in Figure 2.8.

One of the most effective treatments for conservative therapy is the use of custom-made orthopedic footwear. Extra-foot footwear significantly reduces foot pain, improves foot functions and is associated with the development of fewer keratotic lesions in older people.

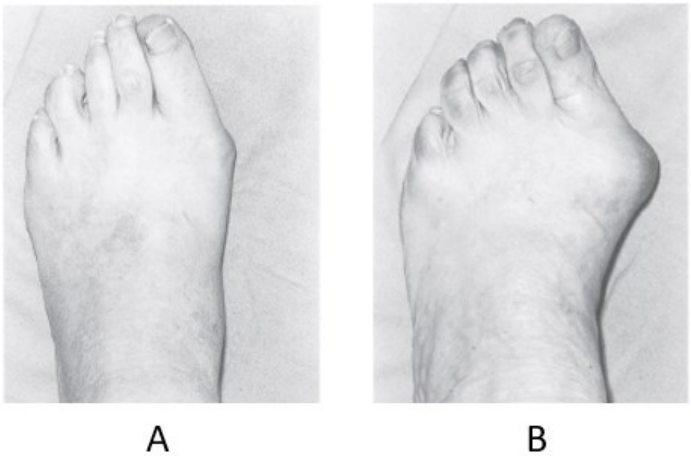


*Figure 2.8: Hallux valgus. (A) Shows a moderate deformity. (B) Shows a severe deformity [7].*

### *2.3.2 Additional pathology with foot deformation effect*

The most common pathologies with foot deformation effects are the rheumatoid arthritis and the diabetes.

**Rheumatoid Arthritis** (RA) is a chronic, inflammatory, autoimmune disease characterized by systemic inflammation, persistent synovitis (inflammation of the synovium, the connective tissue that lines the inside of the joint capsule) and progressive articular destruction [14].

During the early stage of RA the foot is the most common site of pathology. Many patients report foot symptoms at initial diagnosis and up to 100% of patients report foot problems within 10 years of disease onset. A Swedish study found 53% of patients reporting foot involvements at disease diagnosis. The forefoot (45%) was more frequently involved than the rearfoot/ankle (17%) and 9 %reported both forefoot and rearfoot symptoms at diagnosis [15].

In the Forefoot, persistent synovitis and continuous loading of the MTPJs result in attenuation of the joint capsule and supporting ligaments. The integrity of the joint is compromised with consequent digital deformities. The rheumatoid forefoot will develop a typical marked hallux valgus type presentation and hammers toe deformities of the lesser toe. Figure 2.9A shows an example of this deformation.

In addiction to that, the distal shift of the fat pad, which usually is located beneath the MTPJs, expose the metatarsal heads to increased pressure resulting in plantar bursae formation causing painful sensation during gait.

The midfoot is not commonly affected on its own but involved as a consequence of the forefoot and rearfoot deformities.

In the rearfoot, the talonavicular and subtalar joints, which are subject to grater mechanical stress, are the most frequently affected. Pes plano valgus (PPV), shown in Figure 2.9B, is the most common gross structural deformity and it is associated to the gradual weakening of ligamentous and tendon structures that support the medial longitudinal arch [14].


*Figure 2.9: Rheumatoid Feet. A shows the most common deformity of the forefoot in RA, B shows the valgus hindfoot deformity in RA [14].*

In addiction to these structural deformities, the rheumatoid foot is at high risk of ulceration. The risk is elevated because of the tendency to vasculitis and the thinning of the skin, and also because of the deformity accompanying the disease, which leads to the development of area of high pressure, both on the dorsal and on the plantar aspects of the foot [16].

The primary non-pharmacological management is represented by orthopedic footwear. In people affected by RA, footwear interventions are associated with reduction of plantar pressure, foot pain, impairment and disability.

In the majority of the cases, footwear with an upper made of soft leather or stretchable textile is very helpful in reducing the pressure on deformed digits and in accommodating the increased width of the rheumatoid forefoot. In case in which joint pain is severe, shoes with rocker sole can be used to reduce the forefoot pain during walking. However, due to the high variability of patient foot deformity, bespoke footwear are specifically prescribed in order to achieve the best result for each patient.

**Diabetes Mellitus** or diabetes is a metabolic disorder that can be divided in four groups. The first is Type 1 diabetes, it consist of a lack of effective insulin and in the absence of insulin treatment, these patients will usually progress to diabetic ketoacidosis. Type 1 diabetes is an autoimmune disorder with lymphocyte T cells attacking insulin-producing beta (β) cells [17].

The second one is Type 2 diabetes characterized by a relative but not absolute lack of insulin. Peripheral tissue becomes insulin-resistant, that is, less sensitive to the effect of insulin. It is accompanied by a β cells dysfunction [17].

In addiction to these two types exists the monogenic diabetes, a middle atypical forms of type 1 or type 2 diabetes that is diagnosticated in patients younger than 25 years, and the secondary diabetes that occurs when there is direct damage, removal or impairment of action of the mass of β cells [17].

In 2015, 415 million people were estimated to have diabetes, more than 90% of whom had type 2 diabetes. It is estimated that this will increase to 642 million by 2040. The lifetime risk of developing a diabetic foot ulcer is between 19% and 34%, and about 50-60% of ulcers develop infection [18].

The diabetic foot is the results of three great pathologies: neuropathy, ischemia and infection. Diabetic neuropathy is a peripheral nerve disfunction that occurs in 60-70% of people affected by diabetes. Neuropathy can affect nerves throughout the body, but particularly those of the feet and legs. It is identified as a key element in the causal pathway to foot ulceration.

The combination of neuropathy with ischemia and infection results in a rapid progression of tissue necrosis which is the characteristics hallmark of the diabetic foot. Due to the fact that a diabetic foot can quickly reach the point of no return with overwhelming necrosis it is vital to diagnose it early and provide rapid and intensive treatment.

A sub classification of the diabetes foot is represented by the neuropathic foot. it is well perfused and has a palpable pulse. However, sweating is diminished, the skin may be dry and prone to fissuring and any callus present tends to be hard and dry. If the callus are neglected, also due to the reduced nervus sensitivity, and an high plantar pressure is present, ulceration develops and necrosis can develop subsequently.

The orthopedic footwear in combination with orthosis can assume a strategical role in the prevention of foot ulceration and consequently necrosis. It can be an essential effect during the first three stages of neuropathic foot.

The first stage is the normal foot and the patient has to wear correct shoes to prevent the foot from developing unnecessary deformity and callus. The second stage is represented by foot with high-risk factor for ulceration. The aim of a bespoke footwear is to maintain the skin intact in case of severe foot deformity. To conclude, the third stage in which bespoke footwear can have positive effect is when the foot presents ulcers. Here, it is essential to prevent the degeneration and the relative necrosis. On this direction bespoke footwear are used to redistribute plantar pressure, protect the vulnerable margins of the foot avoiding frictional forces by manufacturing shoes with sufficient length, broad and deep [17].

However, after the third stage, the level of necrosis will be such that proper footwear will no longer have the effect necessary to prevent progressive degeneration. For this reason further treatment will be required.

An example of second and third neuropathic foot is show in Figure 2.10.


*Figure 2.10: Neuropathic Foot. (A) Shows a second stage Neuropathic Foot. (B) Shows a third stage Neuropathic Foot [17].*

## 2.4 Duna S.r.l.

The company Duna S.r.l. designs, manufactures and sells with its own brand orthopedic footwear prepared and therapeutic for women, men and children, both mass-produced and custom-made. With its industrial plant located in Falconara Marittima, has always focused on innovation and quality research, with a production able to offer the best solutions to all kinds of problems, combining grade functional effectiveness and attention to aesthetics.

Duna is today a national market leader, one of the major European players in the market, and operates directly or through its distributors in more than 12 countries.

Duna constantly invests in technological research oriented to the creation and development of new products that are tested both by the medical and orthopedic world and in the innovation of its industrial processes in the field of orthopedic footwear.

The company has always believed in the technology to improve its production processes. Thanks to Duna's partnership with important public and private research centers in challenging projects, the possibility of having a built-in technology to support these processes is now a reality.

The technology is the turning point to improve the ability to satisfy not only the customer's demands in terms of aesthetic rendering but also and especially in terms of walking functionality and therapeutic purpose [19].

### *2.4.1 Technological process for customized footwear*

**OrthoShoe** process represents the technology vision of Duna S.r.l. in the field of customization of orthopedic footwear. It includes all the hardware and software tools developed by Duna's Innovation & Technology with the aim of improving the workflow between the orthopedic technician and the production center ensuring the patient a high quality production in a short time.

Figure 2.11, shows a block scheme of the process from the orthopedic shop to the order acquisition in Duna S.r.l.

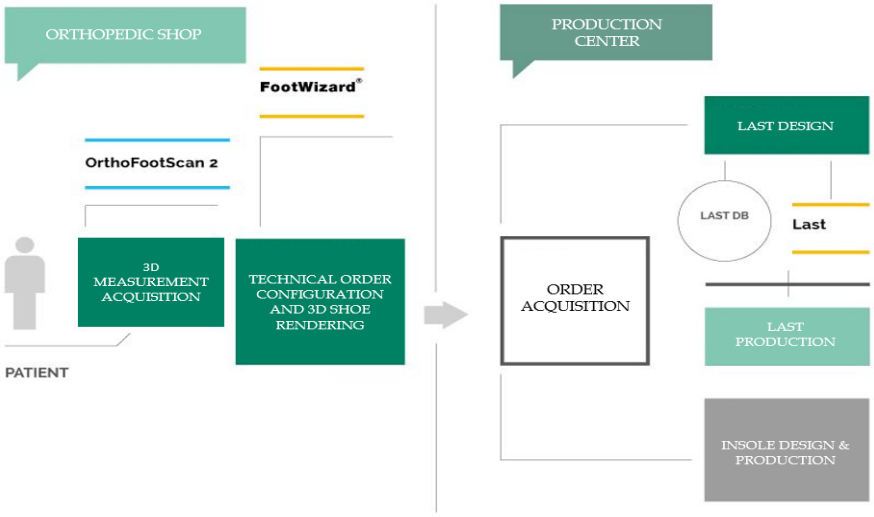


*Figure 2.11: OrthoShoe Process. It shows the order flow from the orthopedic shop to the production center. The image is property of Duna Innovation and Technology [19].*

The creation of a high quality custom-made orthopedic shoe starts in the orthopedic shop. Here, the technician thanks to the **OrthoFootScan 2** acquires the 3D full foot digitalization. It is a mixed stereo-cameras and blue laser technology, that allow a very fast and high level of accuracy. In this way the technician avoids all the mistakes typically of the manually taken measurement and from the digitalization is possible to make an orthopedic customized last with the same accuracy obtained using a foot cast.

The Foot3D software supplied with the scanner, allows to detect the characteristic girths across the foot in a very friendly way and to export the 3D digitalization in Stereolithography (*.stl) format, making the system opened towards any CAD platform.

Once the data acquisition is concluded, it is necessary to have the maximum completeness of the data sent to the production center as well as a clear technical configuration. To achieve this goal, Duna developed **FootWizard R4**.

FootWizard R4 is a unique system to ensure a complete technical configuration and management of the order in the production center for the manufacturing of customized footwear and insoles. It allows a 3D realistic visualization of the final product, starting from individually taken measurement.

It is a platform that can be equipped with three modules: **Custom** for individual personalization, **Modular** for modular shoes personalization and **Insole** for insoles personalization [19].

FootWizard Custom is the module used from the orthopedic technician for the technical and administrative management of the custom-made footwear. Thanks to this system the technician is guided during the acquisition avoiding mistakes and wrong interpretation, speeding up the workflow and reducing operative costs.

At this point the order is sent to the production center and here it is acquired by the Custom Technical Office that translates the inputs provided by orthopedics into design specifications.

In the manufacturing of footwear, the shoe last is the most important structural element. Duna has developed a proper CAD Rhinoceros plug-in for the digital creation of the shoe last: **Last Designer**. It comes from the necessity to develop a software able to optimize internal processes oriented to design customized shoes.

It allows the realization of a CAD last design starting from the acquisition of a cloud-points through a 3D scanner, from manually taken measurement or directly from a positive foot cast implementing automatic algorithms that summarize the experience of Duna's shoe last craftsman. It includes a continuously updated database of last of pathological foot that gives the possibility to design a customized last easily and using few commands.

Once the structure design department has developed the last that ensures compliance with both the pathological characteristics of the subject and the stylistic canons of the shoe chosen, the file generated for the couple of shapes is transferred to the internal Footbed Department, responsible for the 3D CAD design and production of footbed, heel reinforcement and benefit sole, and to the external last production company that realize the physical last.

The physical last is now used for the production of the insole of assembly from the Last and Insole department. It is a building element with the same volume of the insole or orthosis that will be equipped in the final product and it is essential to achieve the required and correct volume inside of the footwear. The materials used to manufacture this element are typically cork and leather.

This department is also responsible for the counter manufacture. After that, the last are sent to the modeling department for the design of the upper and toe cup and subsequently to the hemming department for the production of these elements. These productive passages are still today strictly manual and handicraft.

Once the upper with the counter and toe cup, the footbed and related element, the last and the insole of assembly are manufactured, these components are assembled around the last so as to begin to create the structure of the final shoe.

The outsole is the last element produced. Duna S.r.l. has an internal Sole Department that starting from the row material manufactures a custom-made sole. After the drying phase the shoe passes to the carding machine that smooth and flatten the bottom surface and at this point the sole is glued with a special machinery.

The last step is the finishing and washing of the shoe and consequent removal of the last. At this point the shoe is carried to the warehouse of the finished products and then sent to the customer.

A block scheme of the productive process of custom-made footwear of Duna S.r.l. is presented in Figure 2.12.

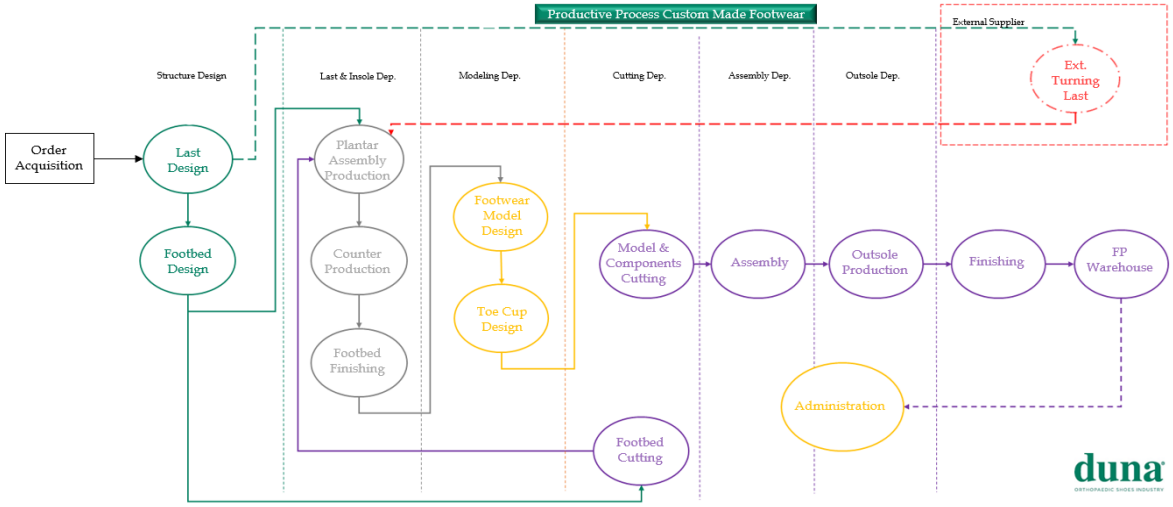


*Figure 2.12: Workflow of a custom-made orthopedic footwear in Duna S.r.l. from the Order Acquisition to the Finite Product.*

# 3 State of the art

During the last decades the product development process of the custom-made footwear was characterized by a strong computerization, starting from the foot diagnosis to the manufacturing of the shoe. Three main stages of action are individualized:

- a foot diagnosis and measurement stage, in which 3D scanners are used to obtain a high quality virtual geometry of the foot;
- a footwear design stage, where all the elements of the shoe are designed using specialized CAD tool;
- a production stage, where CNC machines or 3D printers are employed to manufacture the shoe components.

## 3.1 Customized Insole

The insole is recognized as the most important corrective and supportive element in the majority of the disease. For this reason, the research seeks to replicate in software design tools the manual operations carried out by experienced shoemakers.

Over the years, research has focused more and more on improving the precision and quality of the insole. In literature CAD systems are available that model insole considering only the foot plantar pressure and foot measurements neglecting the 3D shape of the last [20]. More advanced tools were proposed considering the design of the digital insole around the digital foot obtained by using 3D scanner but at the same time achieving the necessary level of control over the orthotics geometry in the form of input parameters. However, these CAD systems fail to satisfy the design of insole for severe deformities such as amputated feet or clubfeet [21].

An additional system that overcame this limited application is presented in [22]. Here, it is developed a virtual prototyping approach based on dedicated foot scanners and CAD-based design tool. The major contribution to design complex insole shapes in this situation come from the involvement of foot scan and highly customized shoe lasts, obtained using dedicated design tools [23].

More advanced approaches combine CAD and CAE systems. The Finite Element Methods were used to simulate the interaction between the insole and the foot, in order to achieve the best geometry and materials combination [24],[25].

From the industrial point of view, several CAD-based solutions are offered on the market. They consist of software tools to design custom-made insoles and aiming at replacing the manual manufacturing processes. The most popular and advanced are paroContour System (by PAROMED) [26], Insole-Designer (by PEDCAD) [27], CANFIT™ INSOLE DESIGN SOFTWARE (by VORUM) [28], IcadPAN (by INESCOP) [29] and Insole Designer (by DUNA s.r.l.) [30].

The first three reported systems are not built on existing CAD but have their own platform. However, this aspect that would seem to simplify the inlay and reduce costs is limited to the design of insole with preventive purpose. In fact, these tools don't require a custom made shoe last as input to the design process but it is sufficient using the 2D scan of the plantar foot. The typical situation, in which they are used, is for insole designed to uniform the foot plantar pressure, avoiding risk of ulcerations and excessive pain, and to add wedges to compensate for leg-length discrepancy.

The IcadPAN and the Insole Designer are CAD applications that run as a plugin to the Rhinoceros CAD system.

INESCOP IcadPAN is able to automatically generate insoles from different input data like foot measurements, the position of foot landmarks, a digital mesh of the foot or scanned insoles or lasts. It is also possible to retrieve data from databases of standard insoles or adapt the insole to a specific last.

The best way of ensuring a perfect fitting to the foot is using scanned foot or mold. However, in some cases pre-generated insoles are available but with the possibility of extra customization to confer the user-defined features. Plantar pressure maps are supported in different formats and they can be used as a guide to design an insole or position additions [29].

DUNA s.r.l Insole Designer creates a complete and accurate 3D nurbs polysurface model. It has a direct connection to the Last Designer software. In particular, the user after designing the shape can import the last directly into the modelling software of the insoles, together with the relative scans of the soles of the feet of the patients so as to create in a few steps the desired orthoses.

Insole Designer, as IcadPAN, has a proper internal database for the standard insoles allowing to reach the final result in a few simple clicks. In complex cases it is possible to adjust the insole starting from the patient's foot, without any restriction or limit to the structures and achievable functionality [19],[30].

What has just been reported shows how in the last two decades, there has been a strong attention and investment of both public and private research on the customization of insole. However, an equally important element for a correct action and effect of the custom orthopedic footwear, at which is not given the same attention, is the footbed.

The footbed is often placed in the background because it seems to be a purely structural element. On the contrary, it is essential to give stability to the shoe and have a proper plantar housing.

## 3.2 Duna's Footbed Production

Duna s.r.l. always focused to the optimization of the production process, has never neglected the computerization and digitalization of the footbed.

Until a few years ago, the company realized this element manually thanks to the presence of high specialized footwear artisans. As a result of the turnover of its staff Duna had to choose whether to recruit a leading figure to the current one or to increase the level of technology and improve the process by moving towards a digitalization of the production process of this component.

Nowadays, Duna has developed a personalized toolbar in the CAD Rhinoceros version 5 called "*Sottopiedi Su Misura*" that facilitates the operator during the design of this element.

The footbed is designed according to specifications directly related to the last on which a particular shoe will be built. In particular, the highly specialized CAD technician, creates a poly-curve following the edge of the lower surface of the digital last that will correspond to the contour of the footbed. An example of the initial profile curve is shown in Figure 3.1.

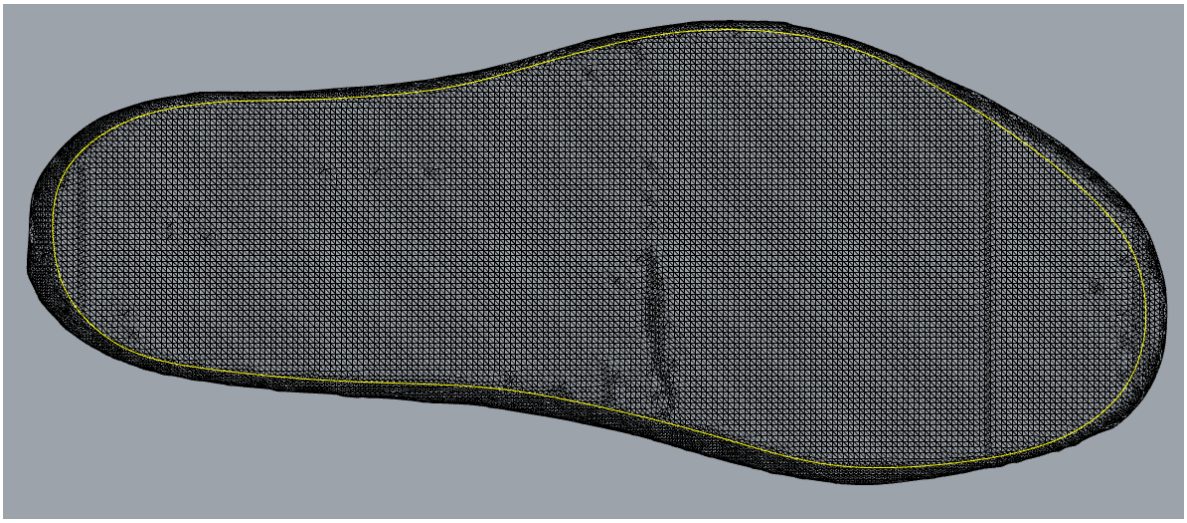

*Figure 3.1: Footbed profile manually designed by Duna S.r.l. CAD technician.*

Once the lateral curve is built, a dedicated command is used to obtain the 3D portion of the mesh corresponding to the footbed. At this point the 3D mesh is flattened into a planar mesh and then the planar curve corresponding to the profile of this element is extracted [31].

An element strictly connected with the design of the footbed is the heel reinforcement. It is not always necessary but if it is required, it is designed during this production phase.

The heel reinforcement design start from the 3D mesh of the footbed. Here, the technician individualizes the medial section corresponding to the diagonal of the metatarsals that delimits the element and draws a straight line, Figure 3.2. At this point all the step described for the design of the footbed are processed also considering this new line.

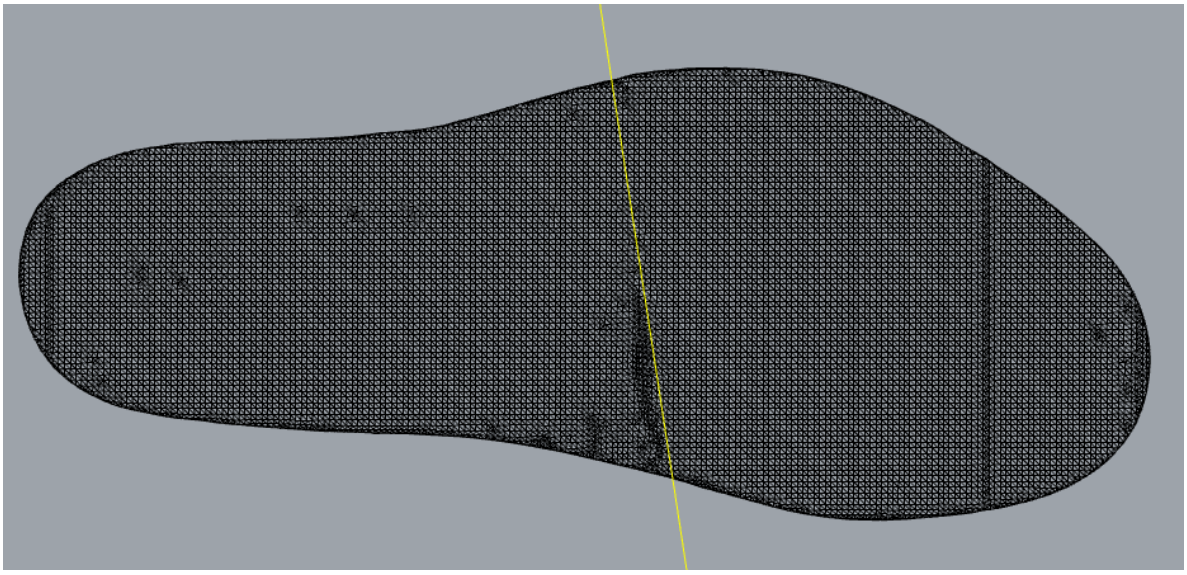

*Figure 3.2:Planar surface of the footbed with the medial line that delimits the heel reinforcement.*

The final result is the profile curve of the footbed intersected by a straight line that crosses it in the medial part, as shown in Figure 3.3.

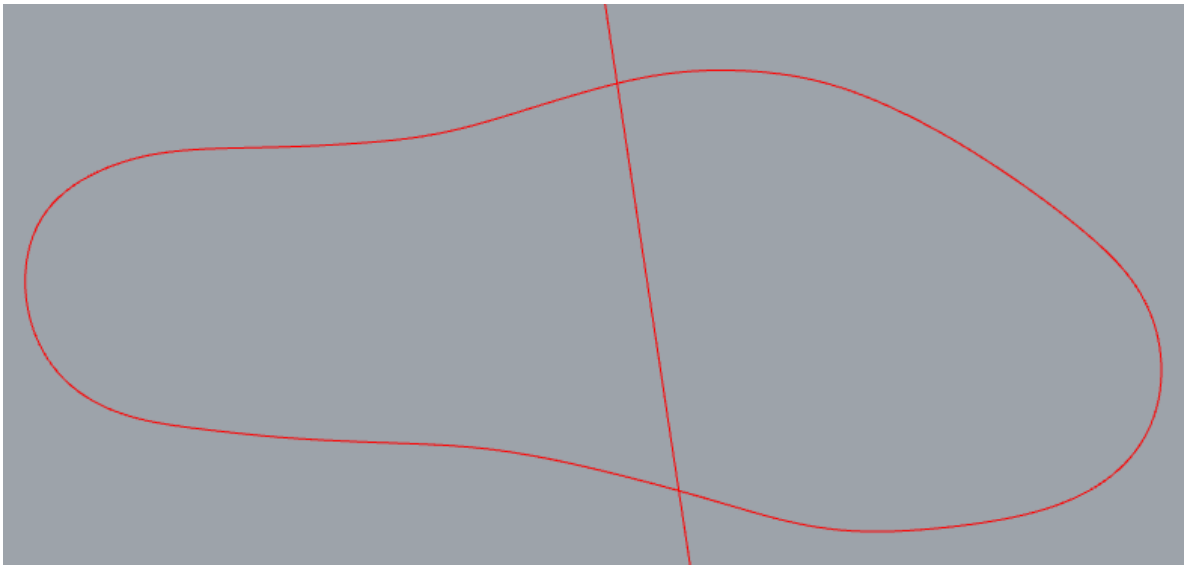

*Figure 3.3: Final Profile curve of the footbed and corresponding medial line for the heel reinforcement.*

Once checked that the measures obtained by the digital procedure correspond to the measures required in reality, the technician makes a copy for the benefit sole (if required), a copy for the footbed and a copy for the heel reinforcement.

At this point the medial line is eliminated from the copies of the footbed and of the benefit sole while in the copy for the heel reinforcement is used to trim the anterior portions of the lateral profile exceeding their intersections.

The last steps are the curves export and the subsequent sending to the cutting bench Nestor.

The main limitation of this procedure is the way in which the initial poly-curve is designed. In fact it strictly depends on the capability of the CAD technician to identify the outer profile of the lower section of the last with a consequent low accuracy and repeatability.

To overcome this limitation, a possible approach could be represented by the integration, within the procedure for the design of these components, of an algorithm capable of extracting automatically or semi-automatically the profile curve of the footbed. The solution could be represented by algorithms, widely studied, for the identification and the automatic extraction of feature lines.

## 3.3 Automatic Feature Lines Extraction Algorithm

Feature line, also known as feature curve, ridge-valley curve or crest line, reveals the main shape properties of surfaces. Recently, digital scanning devices become increasingly popular to capture the surface data from real-world objects. Current scanners are capable of generating a variety of raw data, which inevitably contain a certain level of noise that oftentimes leads to corrupted or bumpy surface meshes.

Over the past decades, feature line extraction gains more and more attention in CAD and computer graphics applications, and hence plenty of methods have been proposed. Among them, a common strategy is to recognize sharp edges or feature points and then connect them to form feature curves [32].

In literature are available a multitude of approaches to identify points and edges characteristics. Some algorithms are based on the identification of the sharp edges by analyzing the adjacent triangles, checking the dihedral angle of their faces, Figure 3.4 [33], or investigating the angle between the normal vectors at the planes fitting the two sides of the investigated edge, Figure 3.5, [34].

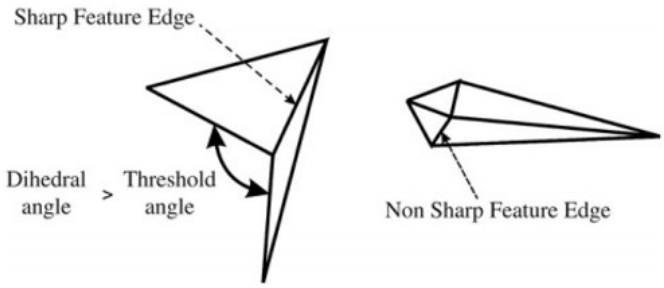


*Figure 3.4: Example of the edges identification approach. Sharp and non-sharp edges. Reproduced from Fig. 7 [33].*

Another approach is based on the estimation of the normal points based on the k nearest neighbors. To detect the significant edges it performs the Delaunay triangulation of the point projected on the least square plane fitting through the normal points [35]. Moreover, to detect feature points to form feature curves the locally estimated mean curvature is considered as the Morse function, a function composed by a network of curves that connect the non-degenerate critical points used to divide the manifold into a collection of regions intrinsically uniform [36]. The majority of these methods achieve satisfactory results on noise-free data respect to the noise one.

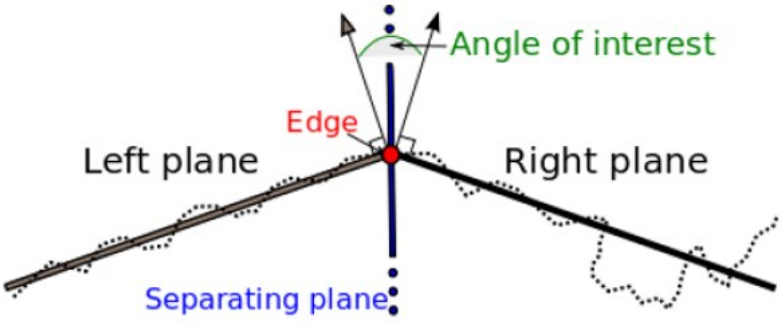


*Figure 3.5: : Estimator for the angle between tangent planes: dotted lines represent the mesh surface (with inliers, outliers and out of region triangles). The estimation of left and right tangent planes depends on a bounding sphere centered at the edge midpoint. Reproduced from Fig. 1 [34].*

In order to obtain a better result in the presence of noise, several incremental methods have been proposed. Some of these algorithms include an initial smoothing of the raw data and subsequently the extraction of the feature lines. In particular, the smoothing is performed with different approaches, such as using a pre-defined scale [37] or computed a smoothing scale for each point of the input model and then applying them at the entire model [38].

Inside of the group of integral methods it is possible to find also the approaches based on the computation of the ridge points and valley points which comprise the feature curves. These points are computed by fitting the local neighborhoods of points using an implicit surface, [38],**Errore. L'origine riferimento non è stata trovata.** or similarly by exploiting an extremity coefficient to check whether a point is a ridge or valley point [1]. This last method combines feature extraction with noise smoothing achieving pleasing result also with a certain level of noise.

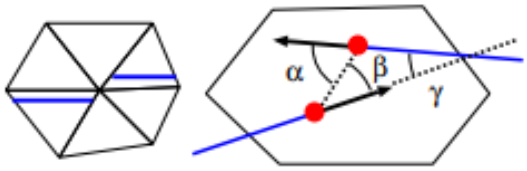


*Figure 3.6: Left: a situation when we may want to connect the crest lines (shown in bold) together. Right: angles a, β, and γ generated by crest line end-segments and the segment connecting crest line end-points are used to measure when gap-jumping is necessary. Reproduced from Fig. 4 [40].*

An additional group of approaches for the feature line extraction is based on sectional curve. One of these approaches is based on the dynamic construction of sectional curves for edges in order to determine the shape edges according to the curvatures of sectional curves [41]. Another one, working directly with a 3D point clouds, constructs a series of sectional curves and subsequently extracts the feature points of those curves to generate feature curves [42]. These methods suffer from noise sensitiveness due to the fact that some thresholds are required to be pre-specified manually, a non-trivial step especially with different level of noise.

An example of characteristic lines automatically extracted is shown in Figure 3.7.

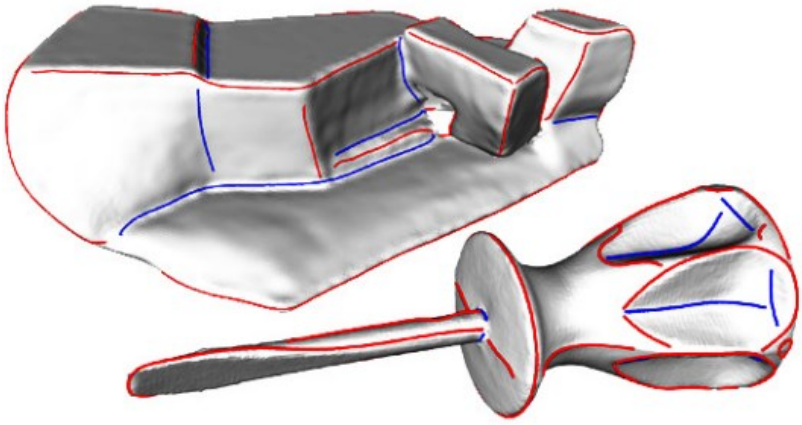

*Figure 3.7: Example of automatic feature lines extraction. Extremality smoothing for high-quality feature line generation works robustly for a large variety of models. Reproduced from Fig. 2 [1].*

All the approaches already presented provide good results with CAD meshes, however none of them has been applied in the footwear industry, especially for the design of components for custom-made orthopedic footwear.

# 4 Methods

The previous section highlighted the lack of software tools to be used for the automatic identification of footbed, heel reinforcement and benefit sole. This work starts from the necessity of the company Duna s.r.l. to develop an algorithm able to extract automatically the profile curve of these elements starting directly from a 3D digital last reducing the intervention of the CAD technician.

The procedure proposed in this work includes three main steps:

- Mesh preprocessing;
- Extraction of feature lines using the algorithm of Hildebrandt et al.;
- Elaboration of the output of the previous step in order to design the curves of the elements of interest.

The algorithm developed involves the use of different software and platforms. In particular, mesh preprocessing is performed using the general purpose 3D CAD system Rhinoceros version 6 in combination with the mesh processing software MeshLab used to convert the file in the suitable format for the feature line extraction algorithm.

The approach of Hildebrandt et al. for feature lines extraction is implemented and developed using the C++ language leveraging the integrated development environment Microsoft Visual Studio 2019.

The output data of the feature line extraction procedure is imported into 3D CAD system Rhinoceros version 6, where they are elaborated in combination with the initial mesh for final curve design.

## 4.1 Mesh typology & Preprocessing

The algorithm is developed to work with three different mesh types:

- Nurbs surface mesh, Figure 4.1A, a mesh obtained starting from the 3D scanning of the foot and built by considering three surfaces above it and fillet together.
- Full scanned digital last, Figure 4.1B, a mesh obtained by scanning a physical last or directly obtained using the Last Design system.
- Scanning the lower portion of a last, Figure 4.1C, using a high performance scanner.

The algorithm is developed around these three types of mesh since, from the beginning, the aim of this work was to develop a robust algorithm and applicable to all the Duna design situations.

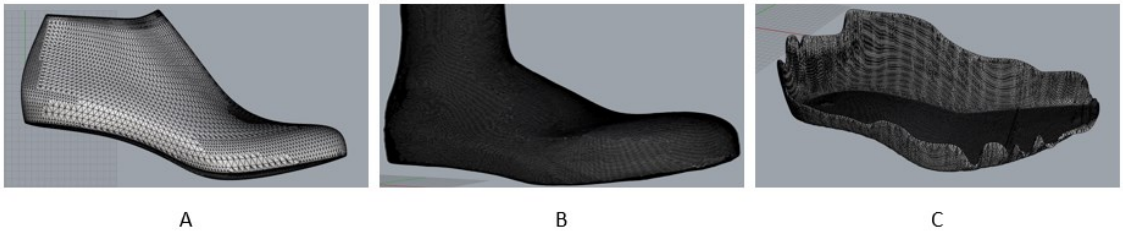


*Figure 4.1: (A) Shows a mesh obtained from Nurbs surfaces, (B) Shown a Full Scanned Digital Last and (C) Shows the scanning of the lower portion of a last.*

Depending on the type of mesh to which the procedure is applied to, the mesh may require a preprocessing necessary to simplify it and make the algorithm as performant as possible. All mesh types are supplied in *.stl format.

If the input of the algorithm is a Nurbs Surface mesh, it is sufficient to create a cutting plane, Figure 4.2A, in order to split the lower part of the last, Figure 4.2B, from the upper useless portion.

In case of a full scanned digital last the preprocessing requires further steps. Before using the cutting plane, Figure 4.2C, to separate the portion of interest, Figure 4.2D, from the excess portion, it is necessary to apply a reduction in the number of mesh triangles and a smoothing of the surface. The Rhinoceros command used to perform these two steps are respectively "*Reduce Mesh*", considering as reducing factor the percentage of reduction set to 50%, Figure 4.3A, and "*Smooth*", using a Smooth factor per step of 0.5 in 2 steps, Figure 4.3B.

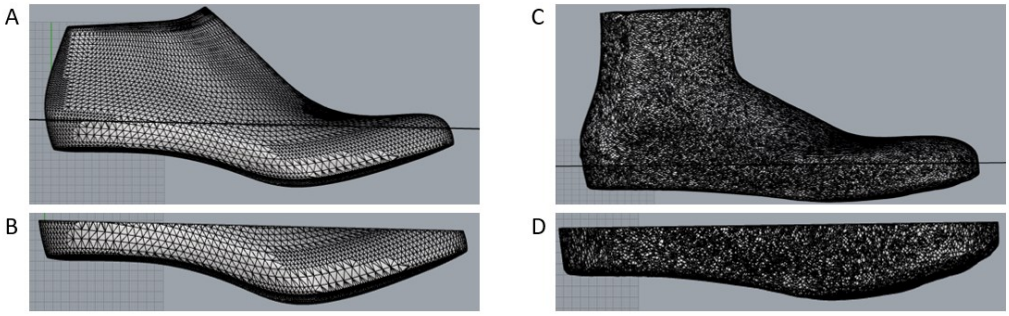


*Figure 4.2: A shows the cutting plane used to isolate the lower portion of a NURBS surface mesh. B shows the lower part coming out from the mesh split with the cutting plane. C shows the cutting plane for the full scanned digital last after the reduction of the number of triangles and the smooth. D shows the lower part coming out from the mesh split with the cutting plane.*

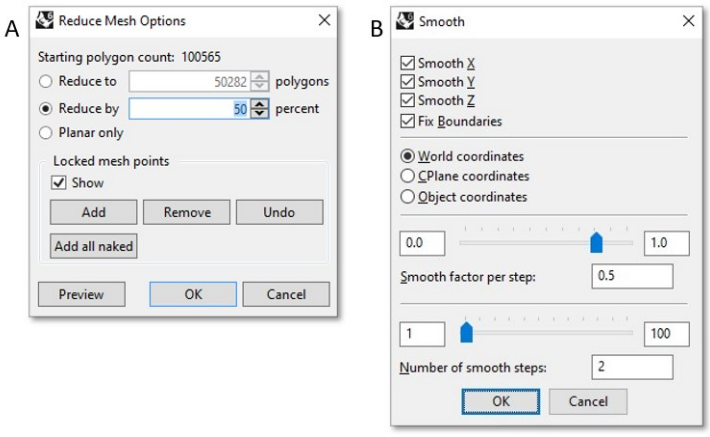


*Figure 4.3: (A) "Reduce Mesh" command option parameters. (B) "Smooth" command option parameters.*

For the third typology of mesh, the scanning of the lower portion of a last, the preprocessing consists in the reduction of the number of the triangles and the smoothing of the surface using respectively the commands "*Reduce Mesh*" and "*Smooth*" with the same option parameters used for the full scanned digital last shown in Figure 4.3. Obviously, in this case, it is not necessary the cutting plane because the mesh presents only the part of interest.

Once the preprocessing is performed, it is necessary to export the new mesh of interest in *.stl format using the dedicated command of Rhinoceros. Subsequently using the Software MeshLab convert the *.stl file into Object File Format (*.off). This step is essential because the algorithm implemented for the feature line extraction require in input a mesh in *.off format.

## 4.2 Smooth Feature Lines on Surface Meshes

To improve the actual methodology based on the high design skills of the specialized CAD technicians, the algorithm of Hildebrandt et al. described in the article "Smooth Feature Lines on Surface Meshes" [1] has been applied to obtain the identification points of the profile curve of the footbed and of the medial line delimiting the heel reinforcement.

The approach described in the article is based on utilizing discrete differential operators on piecewise linear meshes to obtain high quality feature lines. It is based on three main contributions:

- Discrete extremality coefficients characterize feature lines.
- Filtering extremalities stabilize the computation and guaranty feature lines of high quality.
- Feature line extraction identified as zeros of a continuous function avoiding fragmentation and gaps that disconnect feature lines.

### *4.2.1 Discrete Extremality Coefficient*

In order to understand the meaning of discrete extremality coefficient it is necessary starting to define the extremality coefficient.

In the differential geometry, shape operator is defined as the negative derivative of the unit normal N vector of a surface: $\boldsymbol{S = -dN}$. For a smooth surface M in $R^3$ with normal field N it is a symmetric tensor field. The points where S is a multiple of the identity map are called umbilic points. Usually, umbilic points are isolated and for all non-umbilic points the Shape Operator has two different eigenvalues $k_{max} > k_{min}$ that identify the Principal Curvature. The eigenspace corresponding to this eigenvalues are the principal curvature line fields.

If $\overrightarrow{k_i}$ is a locally-defined unit tangent vector field along a curvature line, then the Extremality Coefficient [43] is defined as in Eq. 1.

Eq. 1 $$\boldsymbol{e_i = \langle \nabla k_i, \overrightarrow{k_i} \rangle}$$

It is important to note that extremalities are not well-defined function on the surface because the choice of the sign of $\overrightarrow{k_i}$ produce an ambiguity of sign of $e_i$.

Given a surface M, the set of all points where one of the $e_i$ vanishes is defined as a set of ridges of the surface M. At this point, the Feature Lines are identified in ridge line that verify two additional requirement respectively for $e_{max}$, reported in Eq. 2, and $e_{min}$, reported in Eq. 3.

Eq. 2 $$e_{max} = 0: \left\langle \boldsymbol{\nabla e_{max}}, \overrightarrow{\boldsymbol{k_{max}}} \right\rangle < \mathbf{0}, |\boldsymbol{k_{max}}| > |\boldsymbol{k_{min}}|$$

Eq. 3 $$e_{min} = 0: \left\langle \boldsymbol{\nabla e_{min}}, \overrightarrow{\boldsymbol{k_{min}}} \right\rangle < \mathbf{0}, |\boldsymbol{k_{min}}| > |\boldsymbol{k_{max}}|$$

If the surface orientation gets flipped, the equation (2) and (3) exchange their roles.

Now it is possible to define what is a Discrete Extremality Coefficient. It is obtain discretizing what already seen and, in detail, projecting the function from the general surface to the individual triangles of the mesh.

The first step is to identify a shape operator based on the individual vertices of the triangles. It is computed by averaging over shape operators based at edges and it is calculated as Eq. 4.

Eq. 4 $$S(p) = \frac{1}{2}\sum_{e \ni p} \langle \overrightarrow{N_P}, \overrightarrow{N_e} \rangle S(e)$$

where $\overrightarrow{N_P}$ is the normal at the vertex p, $\overrightarrow{N_e}$ is the edge normal (the average over the normal of the two triangles incident to e) and $S(e)$ is the shape operator at e.

S(p) is a symmetric tensor 3x3 and its eigenvalues, with the biggest absolute value, identify the discrete principal curvature $k_{max}(p) \geq k_{min}(p)$. Let $\overrightarrow{k_{max}}(p)$ and $\overrightarrow{k_{min}}(p)$ be corresponding unit length eigenvectors. As in the smooth case the sign of these vectors is not uniquely.

In order to obtain piecewise linear function, the principal curvatures need to be rescaled with the vertex-based lumped mass matrix.

The gradient of a piecewise linear function, a piecewise constant quantity, is triangle-based. Therefore, for each triangle T and each vertex $p \in T$, $\langle \boldsymbol{\nabla k}_i(T), \overrightarrow{\boldsymbol{k}_\iota}(\mathrm{p}) \rangle$ is a well-defined (up to the choice of the sign of $\overrightarrow{\boldsymbol{k}_\iota}(\mathrm{p})$) constant expression. To obtain the corresponding piecewise linear function, let Eq. 5.

Eq. 5 $$e_i(p) = \frac{1}{area\ (star(p))} \sum_{T \ni p} area(T) \langle \boldsymbol{\nabla k}_i(T), \overrightarrow{\boldsymbol{k}_\iota}(\mathrm{p}) \rangle.$$

Ridge lines are zeros of the discrete extremalities $e_i$, which by definition are linear on each triangle T = ($p_1$, $p_2$, $p_3$). With the discrete situation the zeros of $e_i$ depend on the choice of sign of three principal curvature direction, one each vertices of the triangle T. So, it is necessary a consistent choice of sign for a meaningful definition on a ridge line crossing T that must be repeated for each triangles of the surface.

Inside of a mesh the algorithm distinguish between two triangles type. A triangle T=( $p_1$, $p_2$, $p_3$) is called regular if the signs of $\overrightarrow{\boldsymbol{k}_\iota}(\mathrm{p1})$, $\overrightarrow{\boldsymbol{k}_\iota}(\mathrm{p2})$ and $\overrightarrow{\boldsymbol{k}_\iota}(\mathrm{p3})$ can be chosen such that these vectors have mutually positive inner products. Such a choice is called consistent. However, a triangle is called singular if it is not regular. For most geometries, the bulk of singular triangles is due to high frequency surface noise producing artificial umbilics [1].

Since Feature lines are without umbilics, it will be convenient to process the mesh first without the singular triangles, called regularized.

To sum up, the characteristic lines are well defined on the regular triangles. They are subsets of zeros of the discrete extremalities $e_i$.

## *4.2.2 Processing Of Triangles*

Once the extremalities are in place, the algorithm analyze at first each regular triangle T=( $p_1$, $p_2$, $p_3$) and it compute the (possibly empty) ridge line segment that each triangle contains.

By definition, the feature lines are those ridge lines which verify the additional requirements of Eq. 2 or Eq. 3. At first it is necessary discretize these two conditions. The Eq. 2 after the discretization became:

Eq. 6 $$\langle \nabla e_{max} , \sum_{p_i \in T} \overrightarrow{k_{max}}(p_i) \rangle < 0$$

Eq. 7 $$\left| \sum_{p_i \in T} k_{max}(p_i) \right| > \left| \sum_{p_i \in T} k_{min}(p_i) \right|$$

If the zero set of $e_{max}$ in T is non empty and Eq. 6 and Eq. 7 are satisfied, a segment of the feature lines corresponding to $e_{max}$ is detected. To detect feature lines corresponding to $e_{min}$, the procedure is the same but instead of considering the discretization of Eq. 2, it is considered Eq. 3.

After the processing of the regular triangles it is necessary to evaluate and process also the singular triangles. By the fact that singular triangles do not allow stable computation of extremalities, the processing of this type of triangle take into account adjacent regular triangles.

The algorithm check, for each edge of the singular triangle T, if the corresponding adjacent triangle T' is regular. In this case, it marks each end point of a segment of a characteristic line in T' on the edge common to T.

When all the three edges of T were inspected, and at least one is marked, the algorithm proceeds with one of the subsequent case:

- Regular case, if there are 2 marked edges. It connects the corresponding marked points inside T.
- Trisector case, if there are 3 marked edges. It considers an additional point in correspondence of the barycenter of T and connect it with the three edge points.
- Start/end case, if there is 1 marked edge. It considers only this point [1].

### *4.2.3 Smoothing Feature Lines*

The algorithm developed by Hildebrandt et al. offers also the possibility of an internal smoothing process. It is a modification of the Laplace smoothing that allow the smooth of extremalities $e_i$ on a surface. It works by smoothing extremalities on the entire mesh and not only on the regularized one.

The extremalities are smoothed in the same manner in which a function is smoothed over a surface. However, the traditional Laplace smoothing can be applied only to smooth functions of the entire surface. Since $e_i$'s are not functions on the entire surface, the Laplace smoothing variation applied here compute the extremalities at each vertex of the mesh by using an arbitrary, but fixed, choice of sign of $\overrightarrow{\boldsymbol{k}_i}$ at each vertex.

With this smoothing the instability due to the fact that extremalities involve third order derivatives of the surface, is counteracted.

### *4.2.4 Feature Line Extraction Output*

The output of the algorithm implemented in Microsoft Visual Studio includes a Viewer, Figure 4.4, that shows the mesh loaded with the corresponding feature lines both ridges and valleys, and a list of coordinate x-y-z of the point that identify these curves.

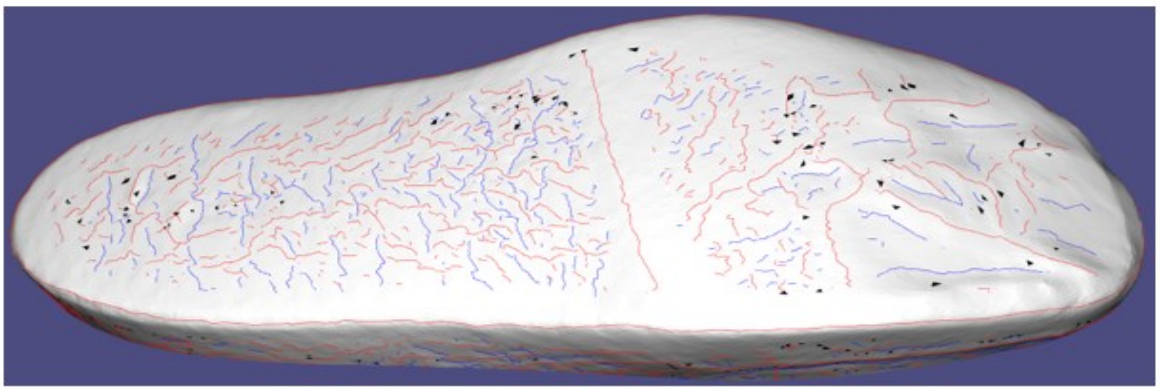

*Figure 4.4: Viewer images. It shows the external view of the last portion. In red the ridges while in blue the valley. Black triangles represent singular triangles. B shows the internal view of the last portion and here are visible only the ridges, in red, and the valleys in blue.*

Since the feature lines of interest in this work correspond to the ridges (red line in Figure 4.4), the algorithm is set to list only the coordinates of ridges points. These points coordinates are saved in a *.txt file.

## 4.3 Design of Footbed, Heel Reinforcement and Benefit Sole.

The final design of footbed, heel reinforcement and benefit sole curves, occurs on the CAD system Rhinoceros. At first the *.txt file, containing the feature points, is imported on the *.3dm Rhinoceros file with the corresponding mesh. From the Figure 4.5, it is possible to see that among the points computed by the algorithm there are many additional points that are not used for the purpose of this thesis work.

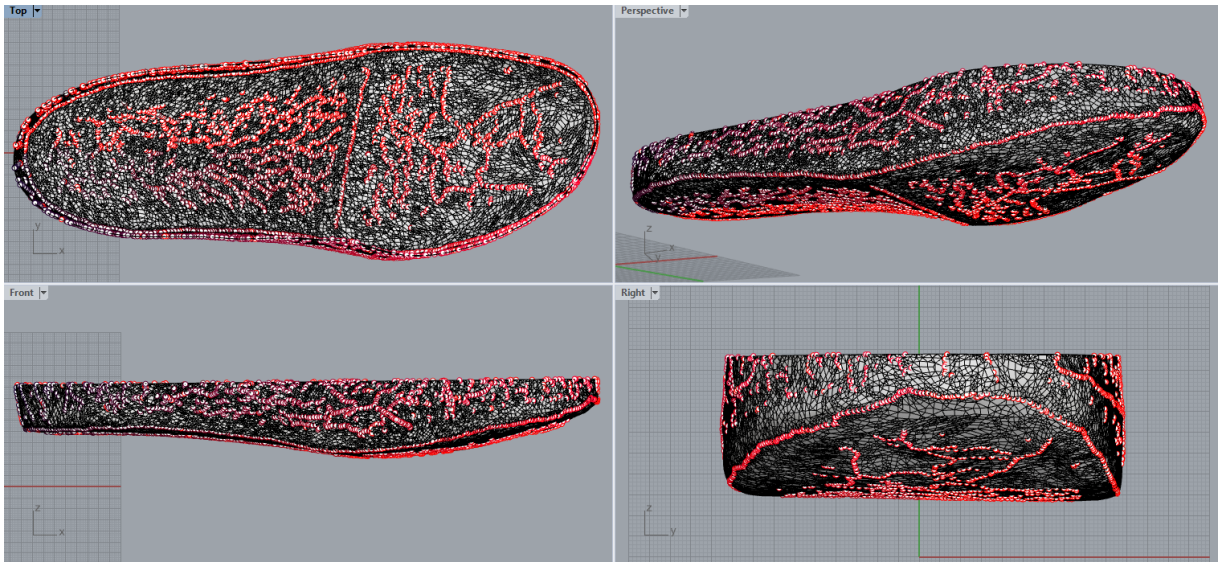


*Figure 4.5: View of the four Rhinoceros planes with mesh and all the feature points extracted from the algorithm.*

For this reason it is necessary to delete all the points in excess respect to the points that characterize the profile curve and the medial line, however visible and easily recognizable. Once this selection is performed, the final result is similar to that shown in Figure 4.6.

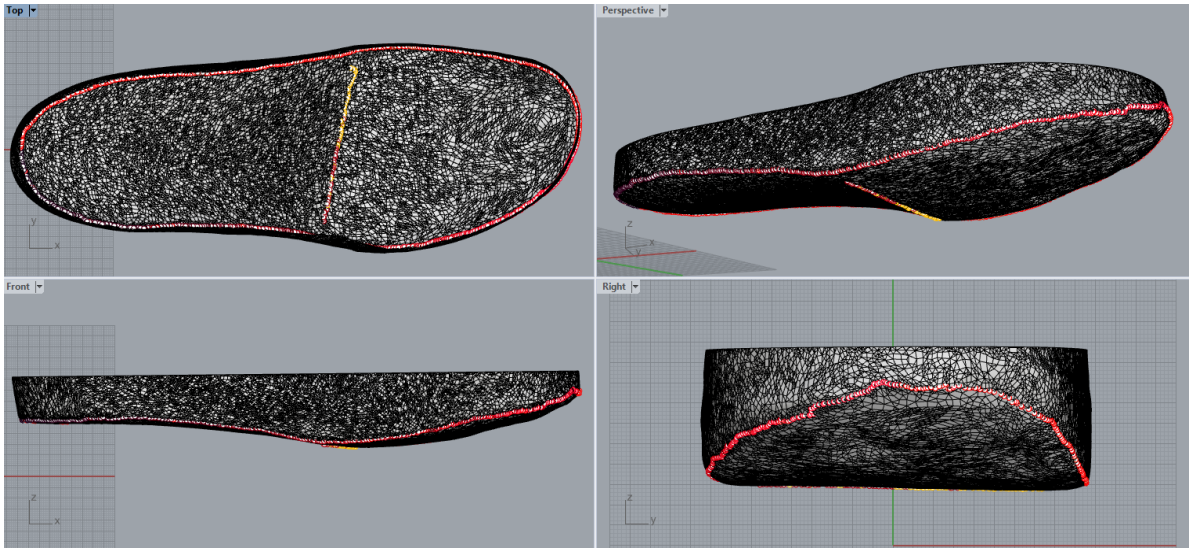


*Figure 4.6: View of the four Rhinoceros planes with the mesh and the points of the profile line and of the medial line after the selection process.*

At this point an initial external profile curve is developed using the command "*Curve Through Pt*". This command require the selection of the points to which build a close curve that in this case correspond only to the lateral points. For what concern the medial points , they are used to design a straight line applying the command "*Line Through Pt*". The lateral curve is the curve from which develop the footbed profile while the medial line is essentially the line used to delimit the hell reinforcement curve.

Before proceeding, the lateral curve need to be rebuild with the dedicated command "*Rebuild*" using the option parameters set to 30 points and 5° degree. After the creation and the reconstruction of the curve, the result is like that in Figure 4.7.

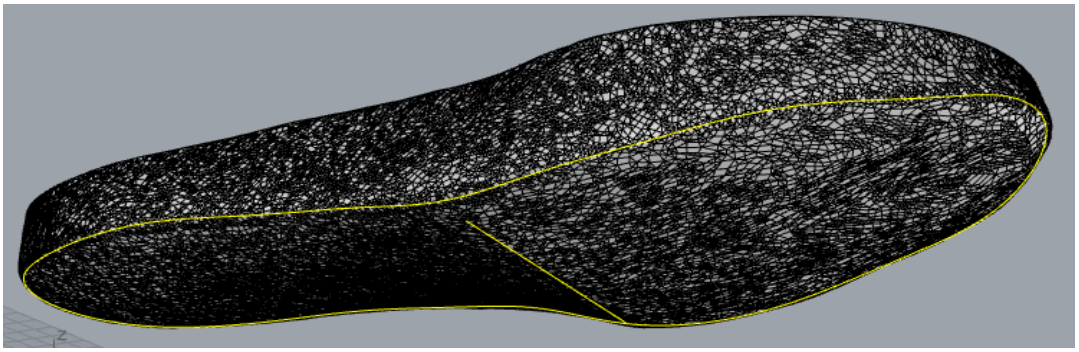

*Figure 4.7: Lateral profile curve after the rebuild and medial line.*

Consider to leave the medial line in the background temporarily and focus only on the lateral profile curve. The goal of this step is to obtain the 3D portion of the mesh that identifies the surface of the last in contact with the footbed.

In order to obtain the above, the profile curve must be extruded conically and at this point divide the mesh with respect to this extrusion. In particular, the extrusion, of 15 mm, is built using the command "Extrude Curve Tapered" using a drift angle of 25° or -25°, keeping attention that the upper surface of the extrusion is smaller than the starting curve as shown in Figure 4.8.

For what concerns the isolation of the 3D surface of the footbed the exceed part is deleted by splitting the actual mesh respect to the extrusion using the command "Mesh Split".

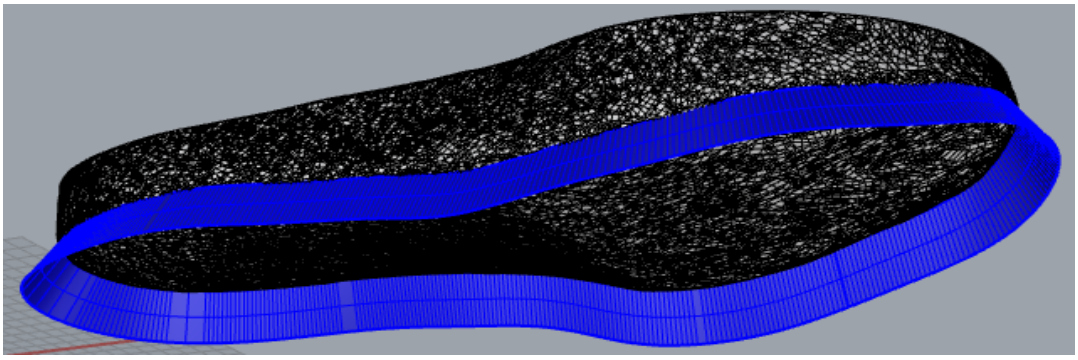

*Figure 4.8: Mesh intersect by the extrusion used to split the 3D footbed surface from the other part.*

Now, since the final profile curve must be a planar curve in order to be cut at the automatic cutting bench, the mesh identifying the footbed must be projected from the current 3D configuration to the 2D one. It is possible to perform using the command "Squish". In this step it is important to squish both the 3D footbed mesh and the medial line, in order to maintain the correct positioning with respect to the mesh.

Keep attention on the plane in which the squish is performed, because for our purpose it is necessary that it is carried out in the top view otherwise the flattening is incorrect.

Once the squish is applied it could be necessary reorient the planar mesh and the curve by using a simple rotation with the correct angulation.

At this point it is necessary only a planar curve and not an entire surface. So, applying the command "Mesh Outline" on the planar surface, it is possible to extract the planar profile curve delimiting the surface as in Figure 4.9.

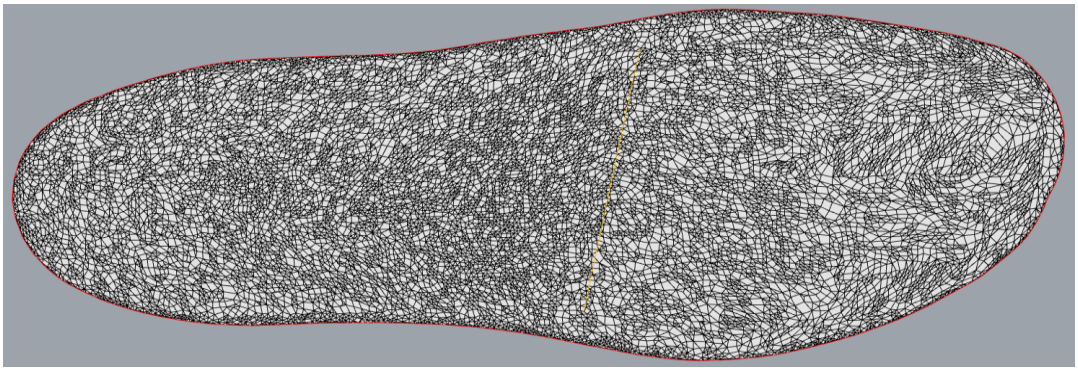

*Figure 4.9: Planar surface of the footbed. In red it is visible the marginal profile curve while in gold the medial line.*

From this situation is now possible to design the final curve for the footbed, heel reinforcement and benefit sole.

In accordance with the order, one, two or three copies of the profile curve and of the medial line are created. Both curve of each copy are reconstructed using the command "Rebuild" with the same parameter of the previous step (30 points and degree 5°). Then the lateral profile curve is offset of 0,5 mm in order to favorite the operator during assembly.

After these elaborations, if the order requires a footbed and a benefit sole, it is sufficient to delete the medial line from the copies corresponding to these two elements. If the order requires also heel reinforcement, two more steps are necessary.

In detail the medial line is connected to the lateral profile curve on both sides using the command “Extend Curve to Boundary” with the specific option “Line” in order to obtain a straight line. Then using the command “Trim” the anterior exceeded portion of the profile curve is deleted and now using “Join” the remaining profile curve and medial line are connected, designing the heel reinforcement profile curve.

The final result if all the elements are required is shown in Figure 4.10.

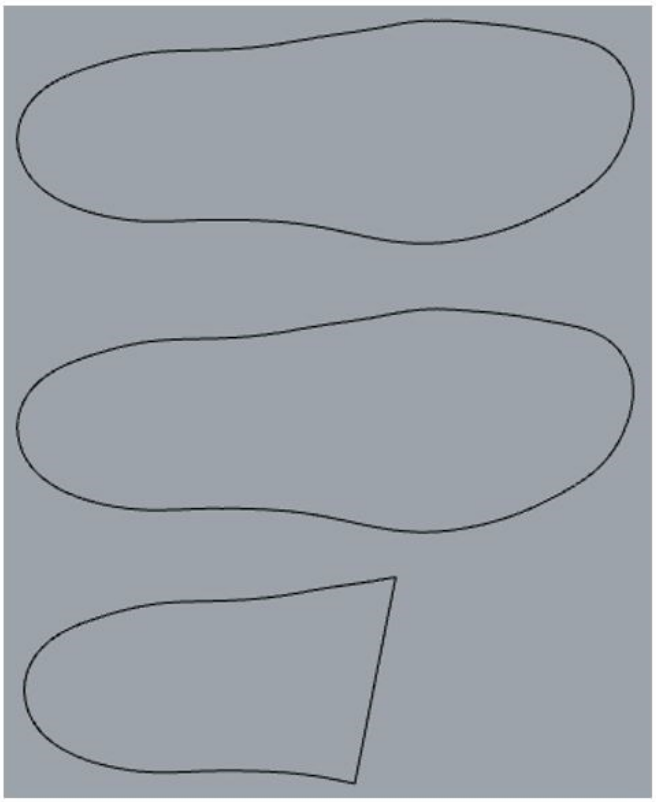

*Figure 4.10: Final Curves. The upper one is the curve of the footbed equal to the middle one that is the benefit sole curve. The lower one is the heel reinforcement curve.*

# 5 Case study

## 5.1 Database

The procedure has been applied to a database of subject lasts provided by the company Duna s.r.l.. The database includes 81 patients for each of which there are scans of both the right and left last for a total of 162 meshes. All the subjects are pathological patients for which a custom-made orthopedic footwear has been prescribed. However, due to the privacy of the patients, the information about the pathology has not been reported for everyone.

All meshes included in the database are scans of the lower portion of the lasts. Since the company provided the scans the use of applying their procedure, a first selection was required. Of the 162 total scans, the procedure was applied to 90 scans.

The selection criteria were exclusively geometrical. Only scans with a complete or nearly complete lateral surface of at least 10 millimeters were considered. An example of scan of the lower portion of last discarded and selected are shown in Figure 5.1.

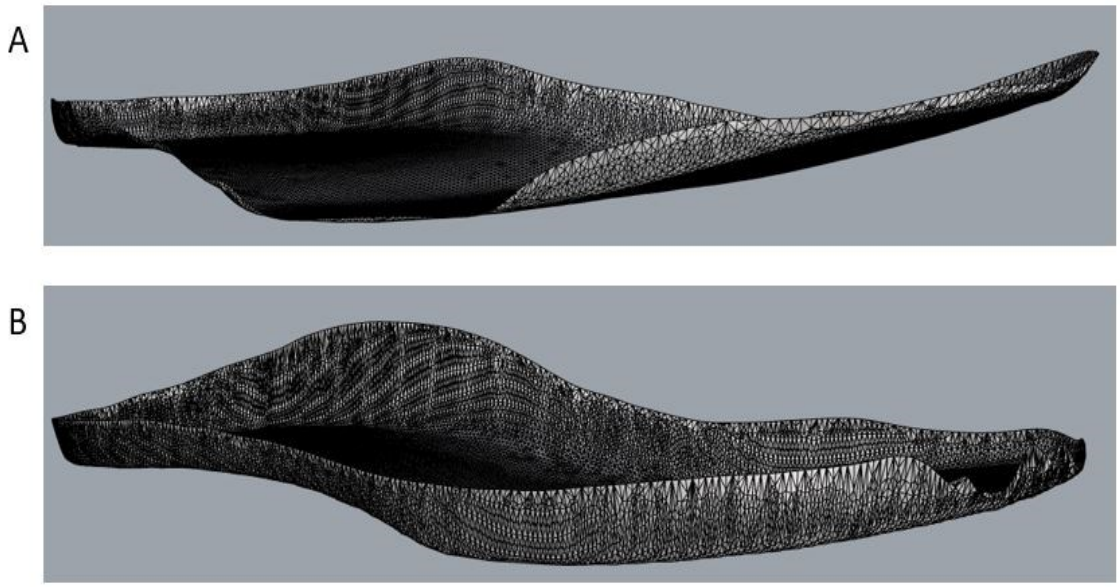


*Figure 5.1: Mesh selection. (A) Shows an example of discarded mesh. (B) Shows an example of mesh to be submitted to the algorithm.*

The 90 suitable meshes were randomly divided into two datasets. The first dataset includes 38 lasts for which the procedure for the design of footbed, heel reinforcement and benefit sole, described in the Method section, was applied without the preprocessing step of triangular reduction and smoothing. The second dataset includes 52 lasts and in this case the procedure described in the previous chapter was applied in its completeness, considering also the preprocessing of the meshes.

The main characteristics of the meshes analyzed are shown in Table 5.1. They are divided between datasets without the preprocessing (Original) and datasets for the complete procedure (Preprocessed).

Table 5.1: Characteristics of the 90 scans of the lower portion of the lasts analyzed.

| | N° | Foot | Mesh Area ($mm^2$) | N° Triangles | Surface of Triangles ($mm^2$) |
|---|---|---|---|---|---|
| Original | 38 | 21 Right<br>17 Left | 33197 ± 8067 | 40776 ± 7918 | 0,81 ± 0,09 |
| Preprocessed | 52 | 25 Right<br>27 Left | 30509 ± 5681 | 18173 ± 2993 | 1,68 ± 0,23 |

The footbed, heel reinforcement and benefit sole, were not designed for all patients but depend on the order received.

The most frequent combination of element was characterized by footbed and heel reinforcement. In some cases all the three elements were required while only for few patients it was required the benefit sole without the other element. Table 5.2 reports all the order configuration of the 90 lasts analyzed.

*Table 5.2: Order configuration for the two Datasets.*

| | Footbed & Heel Reinforcement | Footbed, Heel Reinforcement & Benefit Sole | Benefit Sole |
|---|---|---|---|
| Original | 36 Lasts | 2 Lasts | None |
| Preprocessed | 41 Lasts | 7 Lasts | 4 Lasts |

For each subject Duna S.r.l. provided in addiction to the *.stl files scans of the lower portion of the lasts, also the file *.3dm with their design procedure and final profile curves of the elements.

## 5.2 Validation

The curves designed by Duna were used for a comparison with the curve designed with the approach already presented. The comparison was performed using the Software Geomagic Qualify version 12 from Geomagic. It allows automatic comparisons between a CAD master model and the built part or object.

During the comparison step, the curves provided by Duna were set as reference while the curves coming out from the new procedure were set as test. The same "Max Deviation" equal to 20 mm was set as control parameter for the overall dataset.

The software allows a 2D analysis between the curves, returning a graphical display and a numerical indicator of the deviation between them. The first one is represented by a color scale with fifteen different colors between which green corresponds to zero set, red to the maximum positive deviation and blue to the maximum negative deviation. For what concerns the numerical indicator, the software compute the maximum positive and negative deviation, the mean of the total positive and negative deviation, and the standard deviation. An example of the software output for a footbed comparison is shown in Figure 5.2.

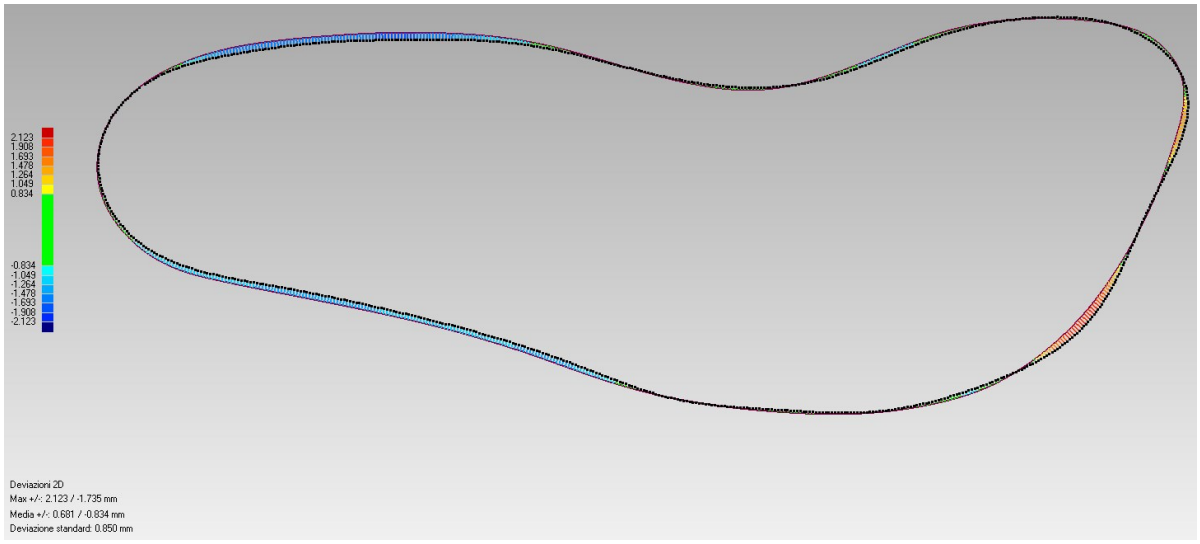


*Figure 5.2: Geomagic Qualify Output. On the left it is visible the color scale. in the middle are reported the two curves with the relative deviation point by point and in the lower left corner there are the numerical indicators.*

After the digital analysis of the profile curves of the component for the 90 scans of the lower portion of the lasts, the company has provided 4 additional meshes belonging to two new patients.

The type of mesh for these patients was full scanned digital last and has been used for an additional trial. The procedure for the semi-automatic extraction of the footbed and heel reinforcement has been applied. After the digital comparison with the curves designed by the CAD technician, has been also performed a physical evaluation.

Once the profile curves have been designed, they have been inserted in the appropriate file with the curves designed by Duna s.r.l. intended for the cutting bench. The resulting leather footbeds and plastic heel reinforcements were physically compared with each other and with the physical last.

# 6 Results & Discussion

The results obtained by the comparison between Duna s.r.l curves and the new approach curves for the two "Original Dataset" and the "Preprocessed Dataset" are reported respectively in Table 6.1 and Table 6.2.

*Table 6.1: Results obtained by the comparison between Duna S.r.l curves and new procedure curves for the "Original Dataset".*

| Sub | Footbed & Benefit Sole | | | Hell Reinforcement | | | |
|---|---|---|---|---|---|---|---|
| | Positive Dev. (mm) | Negative Dev. (mm) | Standard Dev. (mm) | Positive Dev. (mm) | Negative Dev. (mm) | Standard Dev. (mm) | Angle (°) |
| 1 | 0,00 | 1,89 | 1,27 | 0,55 | 1,49 | 0,77 | 1,71 |
| 2 | 0,36 | 1,18 | 0,86 | 1,40 | 2,61 | 1,85 | 8,90 |
| 3 | 0,00 | 2,56 | 1,12 | 0,68 | 2,74 | 1,08 | 3,04 |
| 4 | 1,15 | 0,71 | 1,16 | 2,24 | 0,87 | 1,90 | 1,44 |
| 5 | 0,02 | 1,92 | 0,73 | 0,48 | 1,86 | 0,81 | 1,77 |
| 6 | 0,00 | 2,24 | 1,28 | 3,09 | 1,42 | 2,27 | 4,92 |
| 7 | 0,03 | 1,99 | 1,17 | 0,09 | 1,51 | 1,06 | 3,23 |
| 8 | 0,00 | 2,93 | 0,60 | 4,08 | 2,05 | 3,51 | 6,03 |
| 9 | 0,44 | 1,40 | 1,09 | 0,96 | 1,71 | 1,43 | 2,11 |
| 10 | 0,00 | 2,33 | 1,57 | 2,02 | 1,29 | 1,51 | 0,21 |
| 11 | 0,67 | 3,21 | 1,38 | 0,00 | 2,65 | 1,64 | 0,48 |
| 12 | 0,00 | 2,44 | 1,16 | 2,08 | 1,54 | 2,06 | 3,32 |
| 13 | 0,00 | 2,55 | 0,88 | 1,13 | 1,56 | 1,52 | 2,07 |
| 14 | 0,56 | 2,03 | 1,44 | 0,57 | 1,73 | 1,54 | 2,33 |
| 15 | 0,00 | 1,89 | 0,69 | 2,45 | 2,07 | 1,92 | 6,08 |
| 16 | 0,00 | 2,90 | 0,62 | 1,85 | 2,02 | 1,83 | 2,21 |
| 17 | 0,00 | 1,90 | 0,48 | 0,10 | 1,36 | 0,69 | 0,60 |
| 18 | 0,00 | 2,13 | 0,73 | 0,90 | 1,19 | 1,12 | 1,10 |
| 19 | 0,01 | 1,73 | 0,75 | 0,80 | 1,52 | 0,79 | 2,73 |
| 20 | 0,00 | 1,97 | 0,78 | 3,95 | 1,77 | 2,40 | 7,07 |
| 21 | 0,00 | 2,29 | 1,15 | 5,23 | 1,92 | 2,92 | 3,02 |
| 22 | 0,00 | 3,02 | 1,03 | 4,10 | 2,31 | 2,47 | 7,84 |
| 23 | 0,60 | 0,73 | 0,84 | 1,04 | 2,27 | 1,88 | 3,38 |
| 24 | 0,74 | 2,08 | 1,43 | 0,63 | 1,96 | 1,60 | 1,60 |
| 25 | 0,26 | 2,97 | 1,14 | 1,03 | 2,75 | 1,63 | 12,63 |
| 26 | 0,62 | 2,06 | 1,05 | 2,63 | 2,12 | 2,66 | 5,63 |
| 27 | 0,00 | 2,76 | 0,80 | 8,14 | 3,49 | 5,28 | 10,44 |
| 28 | 0,25 | 1,82 | 1,09 | 0,62 | 2,07 | 1,40 | 1,68 |
| 29 | 0,00 | 2,75 | 1,25 | 1,07 | 2,26 | 1,52 | 4,72 |
| 30 | 1,18 | 0,80 | 1,11 | 1,19 | 0,65 | 1,17 | 3,54 |
| 31 | 0,00 | 2,33 | 1,19 | 0,06 | 1,31 | 0,56 | 1,27 |
| 32 | 0,00 | 2,32 | 1,02 | 0,90 | 1,92 | 1,22 | 1,82 |
| 33 | 0,00 | 1,91 | 0,97 | 0,52 | 1,90 | 0,85 | 2,03 |
| 34 | 0,00 | 2,75 | 1,22 | 0,93 | 1,59 | 1,33 | 1,35 |
| 35 | 0,00 | 2,41 | 0,56 | 0,73 | 1,96 | 1,22 | 1,83 |
| 36 | 0,00 | 2,27 | 0,89 | 0,36 | 2,25 | 0,90 | 1,97 |
| 37 | 0,00 | 2,62 | 0,96 | 1,22 | 1,92 | 1,61 | 2,64 |
| 38 | 0,04 | 2,36 | 1,09 | 2,10 | 2,05 | 1,52 | 6,86 |

*Table 6.2: Results obtained by the comparison between Duna s.r.l curves and new procedure curves for the "Preprocessed Dataset".*

| Sub | Footbed & Benefit Sole | | | Heel Reinforcement | | | |
|---|---|---|---|---|---|---|---|
| | Positive Dev. (mm) | Negative Dev. (mm) | Standard Dev. (mm) | Positive Dev. (mm) | Negative Dev. (mm) | Standard Dev. (mm) | Angle (°) |
| 1 | 0,21 | 1,24 | 0,93 | 1,10 | 0,92 | 1,21 | 2,72 |
| 2 | 0,42 | 1,19 | 0,93 | 0,85 | 1,73 | 1,72 | 5,13 |
| 3 | 0,00 | 1,65 | 0,66 | 1,96 | 1,11 | 1,61 | 3,56 |
| 4 | 0,48 | 1,07 | 0,84 | 1,33 | 1,03 | 1,32 | 2,33 |
| 5 | 0,00 | 1,58 | 0,74 | 0,88 | 1,23 | 1,08 | 2,72 |
| 6 | 0,67 | 1,29 | 1,29 | 2,28 | 1,91 | 3,90 | 0,19 |
| 7 | 0,95 | 0,72 | 0,88 | 0,44 | 0,76 | 0,67 | 0,12 |
| 8 | 0,68 | 0,83 | 0,85 | 0,89 | 0,95 | 0,99 | 0,75 |
| 9 | 0,27 | 0,97 | 0,69 | 1,67 | 0,67 | 1,43 | 0,63 |
| 10 | 0,56 | 1,14 | 0,86 | 0,77 | 0,67 | 0,83 | 1,26 |
| 11 | 0,38 | 1,01 | 0,82 | 1,69 | 0,98 | 1,39 | 5,80 |
| 12 | 1,50 | 1,02 | 1,65 | 1,65 | 0,68 | 1,27 | 2,23 |
| 13 | 0,63 | 1,06 | 0,68 | 0,96 | 0,84 | 0,94 | 3,30 |
| 14 | 0,67 | 0,98 | 0,88 | 1,43 | 0,82 | 1,03 | 0,38 |
| 15 | 1,28 | 1,28 | 1,11 | 0,96 | 0,98 | 0,91 | 2,33 |
| 16 | 0,43 | 1,28 | 0,80 | 1,10 | 1,38 | 1,21 | 2,96 |
| 17 | 0,68 | 0,71 | 0,82 | 1,66 | 0,91 | 1,71 | 4,85 |
| 18 | 0,35 | 1,53 | 1,24 | 0,45 | 0,74 | 0,67 | 1,21 |
| 19 | 0,27 | 0,78 | 0,69 | 0,55 | 0,78 | 0,70 | 1,21 |
| 20 | 0,50 | 0,73 | 0,79 | 0,51 | 0,82 | 0,81 | 1,94 |
| 21 | 0,46 | 0,74 | 0,70 | 0,25 | 0,85 | 0,59 | 0,48 |
| 22 | 0,02 | 1,16 | 0,80 | 0,47 | 0,87 | 0,93 | 3,97 |
| 23 | 0,41 | 0,88 | 0,76 | 0,34 | 0,83 | 0,77 | 2,82 |
| 24 | 0,21 | 1,24 | 0,93 | 0,95 | 1,10 | 0,87 | 2,97 |
| 25 | 0,05 | 1,67 | 1,10 | 1,13 | 1,27 | 1,61 | 1,88 |
| 26 | 0,19 | 1,69 | 0,74 | 0,53 | 1,28 | 0,95 | 0,46 |
| 27 | 0,25 | 1,21 | 1,04 | 0,84 | 1,11 | 1,17 | 0,79 |
| 28 | 0,36 | 1,19 | 0,66 | 0,00 | 1,49 | 0,46 | 0,46 |
| 29 | 0,16 | 1,57 | 0,90 | 1,18 | 2,11 | 1,83 | 11,73 |
| 30 | 0,66 | 1,27 | 0,83 | 0,48 | 1,24 | 0,81 | 1,03 |
| 31 | 0,30 | 1,35 | 0,81 | 0,69 | 1,32 | 1,27 | 0,83 |
| 32 | 0,23 | 1,23 | 0,77 | 1,82 | 1,88 | 1,39 | 8,13 |
| 33 | 0,04 | 1,51 | 0,74 | 2,04 | 1,32 | 1,91 | 2,69 |
| 34 | 0,17 | 1,40 | 0,71 | 0,29 | 0,99 | 0,68 | 1,72 |
| 35 | 0,45 | 0,71 | 0,65 | 0,34 | 0,72 | 0,65 | 2,47 |
| 36 | 0,35 | 1,75 | 1,01 | 0,36 | 2,07 | 1,02 | 2,62 |
| 37 | 0,42 | 1,34 | 0,97 | 2,73 | 1,27 | 1,87 | 8,47 |
| 38 | 0,56 | 1,40 | 0,98 | 0,80 | 1,41 | 1,23 | 1,56 |
| 39 | 0,00 | 1,29 | 0,72 | 5,16 | 1,94 | 2,28 | 14,68 |
| 40 | 0,27 | 1,74 | 0,84 | 2,65 | 1,73 | 2,36 | 4,10 |
| 41 | 0,69 | 0,82 | 0,71 | 0,96 | 1,10 | 1,13 | 3,27 |
| 42 | 0,76 | 1,15 | 0,95 | 0,23 | 1,51 | 0,89 | 1,98 |
| 43 | 0,05 | 2,01 | 1,08 | 1,68 | 1,69 | 1,85 | 1,67 |
| 44 | 0,00 | 0,87 | 0,48 | 0,41 | 0,76 | 0,73 | 0,89 |
| 45 | 0,66 | 0,72 | 0,75 | 1,03 | 0,62 | 1,00 | 2,69 |
| 46 | 0,50 | 0,80 | 0,67 | 0,73 | 0,92 | 0,71 | 0,20 |
| 47 | 0,42 | 1,16 | 0,83 | 2,45 | 1,35 | 2,41 | 6,12 |
| 48 | 1,07 | 1,13 | 1,26 | 0,33 | 1,08 | 0,83 | 2,12 |
| 49 | 1,85 | 1,15 | 1,17 | NN | NN | NN | NN |
| 50 | 0,01 | 1,49 | 0,72 | NN | NN | NN | NN |
| 51 | 1,66 | 1,45 | 1,46 | NN | NN | NN | NN |
| 52 | 0,31 | 1,35 | 0,78 | NN | NN | NN | NN |

Mean deviations, both positives and negatives, and standard deviations are reported for the footbed, benefit sole and heel reinforcement comparisons. In addition, the angles between the medial line of the two procedures used to delimit the heel reinforcement are outlined.

The mean deviation and the standard deviation were considered as the most significant values among the data provided by the software Geomagic Qualify, used for comparing the curves designed by Duna s.r.l. and those obtained with the new methodology. The maximum deviations were discarded because the alignment between the two curves compared have been performed manually. Thus, it was an insignificant value.

From a statistical point of view, the results of the comparison performed on the curves designed for the orders, for which only benefit sole was prescribed, are listed under the same columns of the footbed data. This choice is related to the fact that the procedure for the design of the footbed and benefit sole is equal until the cutting moment. In particular these cases are observable in the last four rows of Table 6.2 where only data for the first four columns are present.

In order to understand how the mean deviation are distributed, some histograms, were created. In the graphs the mean positive and negative deviations are distributed over five set of millimeters deviation, ranging from 0 to 2 mm. In particular for each dataset were built two histograms respectively for footbed & benefit sole together, and heel reinforcement. The distribution for the original and preprocessed datasets are shown respectively in Histogram 6.1 and **Errore. L'origine riferimento non è stata trovata.**.

In blue are represented the positive deviation while in orange the negative one. It is important to consider that each curves analyzed has both positive and negative deviation.

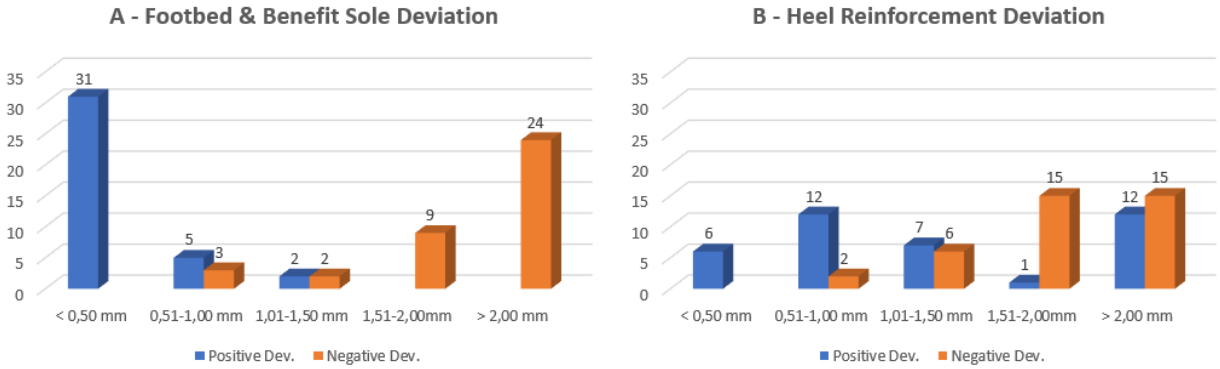


*Histogram 6.1: Distributions of the mean positive and negative deviations of the "Original Dataset". (A) reports the mean deviation for Footbed & Benefit Sole curves. (B) reports the mean deviation for Heel Reinforcement curves.*

From Histogram 6.1A it is possible to note that in the Original Dataset, the distribution of the positive deviation of footbeds is concentrated around the first two range of deviations, respectively 81% near zero and 13% between 0,51 and 1,00 mm. In contrast, the negative deviation of footbeds are distributed around the last two ranges, 23% between 1,51 and 2,00 mm and the 63% more than 2,00 mm .

Observing the histograms of the heel reinforcement, Histogram 6.1B, it is possible to note how the positives and negatives deviation are widely distributed around all the ranges of deviations also if in different percentage.

The 31% of the curves show a positive deviation between 0,51 and 1,00 mm and another 31% more than 2,00mm, and contemporary the 39% show a negative deviation between 1,51 and 2,00 mm and the same percentage more than 2,00mm.

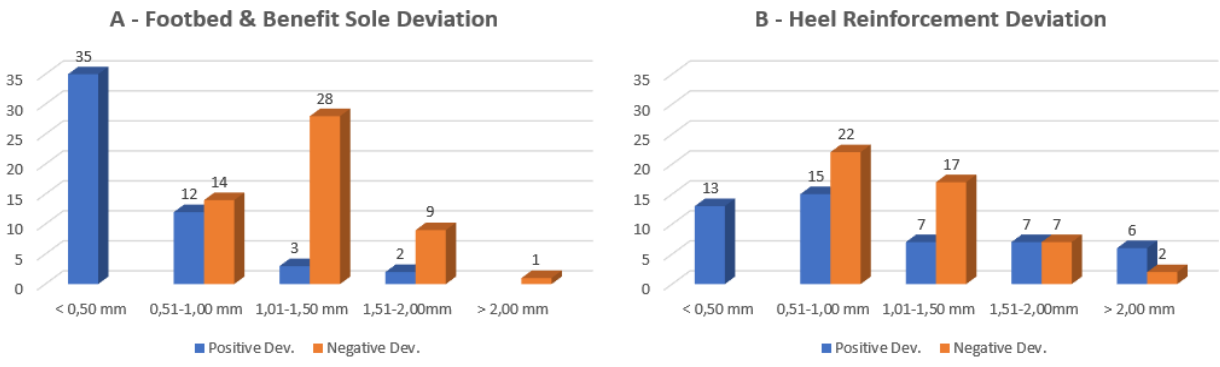


*Histogram 6.2: Distributions of the mean positive and negative deviations of the "Preprocessed Dataset". (A) reports the mean deviation for Footbed & Benefit Sole curves. (B) reports the mean deviation for Heel Reinforcement curves.*

For what concerns the footbed deviation of the Preprocessed Dataset, the positive deviation shows a trend similar to the previous one with the 67% near zero and 23% between 0,51 and 1,00 mm, while the negative deviation is distribute around three ranges of deviation: the 26% between 0,51 and 1,00 mm, the 53% between 1,01 and 1,50 mm and the 17% between 1,51 and 2,00 mm.

Observing the histograms of the heel reinforcement, Histogram 6.2B, the positive deviation are distributed around all the ranges with the higher concentration in the range near zero, the 25%, and in the range between 0,51 and 1,00mm, the 28% while the negative deviations are mainly concentrated in the range 0,51-1,00 mm, the 42%, and in the range 1,01-1,50 mm, the 32%.

By comparing the histograms of the same footwear element obtained for the two different datasets, it is possible to note that for the footbed and benefit sole the positive deviation is lower than 1 mm for the majority of the curves designed, while the negative deviations distribution has a completely different behavior between the two meshes groups.

From this configuration of the results it is possible to appreciate how the footbed and benefit sole designed with the new approach deviate from the curves of the same elements designed by Duna s.r.l. in a systematic way. However, this systematization is lost in the design of the heel reinforcement.

For a better understanding of the results the mean of the mean deviation and their standard deviation were computed for both the dataset. In addiction, the mean absolute deviation were computed as the mean of the sum of both positive and negative deviation for each mesh analyzed. The results obtained are shown in Table 6.3.

*Table 6.3: Mean value of the mean deviations, both negative, positive and absolute, relative Standard deviation for Footbed, Benefit Sole and Heel Reinforcement and mean angle deviation of the medial line of heel reinforcement.*

| | **Footbed & Benefit Sole** | | | **Heel Reinforcement** | | | |
|---|---|---|---|---|---|---|---|
| | Positive Dev. (mm) | Negative Dev. (mm) | Absolute Dev. (mm) | Positive Dev. (mm) | Negative Dev. (mm) | Absolute Dev. (mm) | Angle (°) |
| Original | 0,18 ± 0,32 | 2,16 ± 0,60 | 2,34 ± 0,49 | 1,63 ± 1,66 | 1,89 ± 0,54 | 3,51 ± 1,89 | 3,57 ± 2,83 |
| Preprocessed | 0,43 ± 0,32 | 1,19 ± 0,32 | 1,69 ± 0,00 | 1,12 ± 0,89 | 1,16 ± 0,40 | 2,25 ± 1,11 | 2,88 ± 2,87 |

From the results just shown, it is possible to note that the curves of footbed and benefit sole obtained for the Original Dataset are characterized by a mean absolute deviation of 2,34 mm with a prevalent negative deviation of approximately 2.16 mm and a positive deviation of 0,18 mm. This means that the curves designed with the new approach are smaller respect to the Duna S.r.l curves of a significant value.

For what concerns the mean deviation of the same element curves designed for Preprocessed Dataset, the mean absolute deviation is 1,69 mm with the mean negative deviation always prevailing of about 1,19 mm, but the mean positive deviation is raised at 0,43 mm . This means that by performing the preprocessing for the reduction of the triangles of the meshes and the smoothing, the curves for the footbed and the benefit sole obtained with the new procedure are still smaller respect to the curves of Duna, but the error is sensitively reduced respect to the previous dataset.

Different results are shown for the heel reinforcements. For this element both the positive and negative deviation are more than one millimeter. The results obtained with the Original Dataset shown a positive mean deviation of 1,63 mm and a negative deviation of 1,89 mm, resulting in a mean absolute deviation of 3,51 mm, while the results obtained with the Preprocessed Dataset are respectively 1,16 mm and 1,24 mm, with a mean absolute deviation of 2,25 mm.

The results of heel reinforcements confirms the fact that, by preprocessing the meshes, the error is reduced. However, the error for this element is already high in both positive and negative deviations. The bigger variation of this element respect to variations of the footbed and benefit sole, could be due to the different medial line identified.

In some cases the presence of the angle variation between the two medial lines designed with the different procedures assume a significant value. This leads to a higher deviation between the element curves. In particular a double trend is appreciable: some curves deviate unilaterally, this means that they show only a high positive or negative deviation, while other curves present contemporary an high positive and negative deviation after the comparison. An example of these two severe conditions are shown respectively in Figure 6.1A and Figure 6.1B.

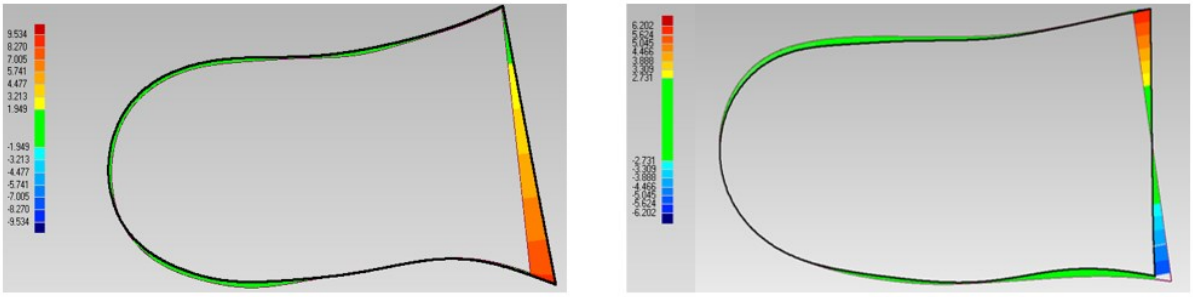


*Figure 6.1: Example of high deviation of the heel reinforcement curve.. It underlines how the different angle of the medial line between the two procedure increase the error. (A) Shows an example of angle deviation that produce an increase of positive deviation. (B) shows an example of angle deviation that provide an increase in both positive and negative deviations.*

However, the examples reported show extremely severe situations that occurs on a limited number of meshes.

The application of the new methodology to the four additional lasts, for which the profile curve of the elements have been physically cut, allows us to understand the real difference between the shoe elements designed with the two different procedures.

Table 6.4 reports the data of the digital comparison of the footbeds and heel reinforcements for the new subjects.

*Table 6.4: Digital comparison results for the new four meshes analyzed. For each mesh it is reported the positive, negative and absolute deviation for the footbed and heel reinforcement and in addiction it is reported also the medial line angle variation.*

| Sub | Footbed | | | | Heel Reinforcement | | | | |
|---|---|---|---|---|---|---|---|---|---|
| | Positive Dev. (mm) | Negative Dev. (mm) | Absolute Dev. (mm) | Standard Dev. (mm) | Positive Dev. (mm) | Negative Dev. (mm) | Absolute Dev. (mm) | Standard Dev. (mm) | Angle (°) |
| 1 | 0,75 | 1,01 | 1,76 | 1,17 | 0,61 | 0,73 | 1,34 | 0,75 | 1,78 |
| 2 | 0,97 | 0,87 | 1,84 | 1,03 | 1,62 | 2,91 | 4,53 | 3,10 | 8,66 |
| 3 | 0,60 | 0,32 | 0,92 | 0,51 | 1,95 | 0,82 | 2,77 | 2,32 | 5,17 |
| 4 | 0,91 | 0,32 | 1,23 | 0,71 | 1,40 | 1,08 | 2,48 | 1,49 | 8,61 |

The physical evaluation was performed by comparing the elements obtain with the two different procedures on the same mesh putting the element designed by Duna S.r.l. above that of the new procedure, and subsequently, comparing them with the physical lasts.

The physical comparisons with the corresponding digital comparisons for the four footbed and heel reinforcement cut, are shown respectively in Figure 6.2, Figure 6.3, Figure 6.4 and Figure 6.5.

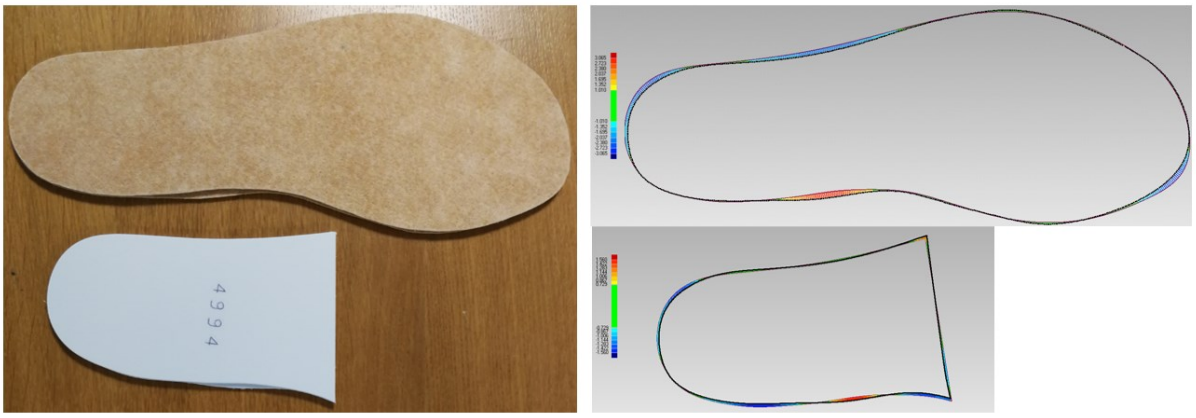


*Figure 6.2: Physical and Digital comparison of Footbed and Heel Reinforcement curve for subject 1 of Table 6.4. On the left is shown the physical comparison while on the right the digital one.*

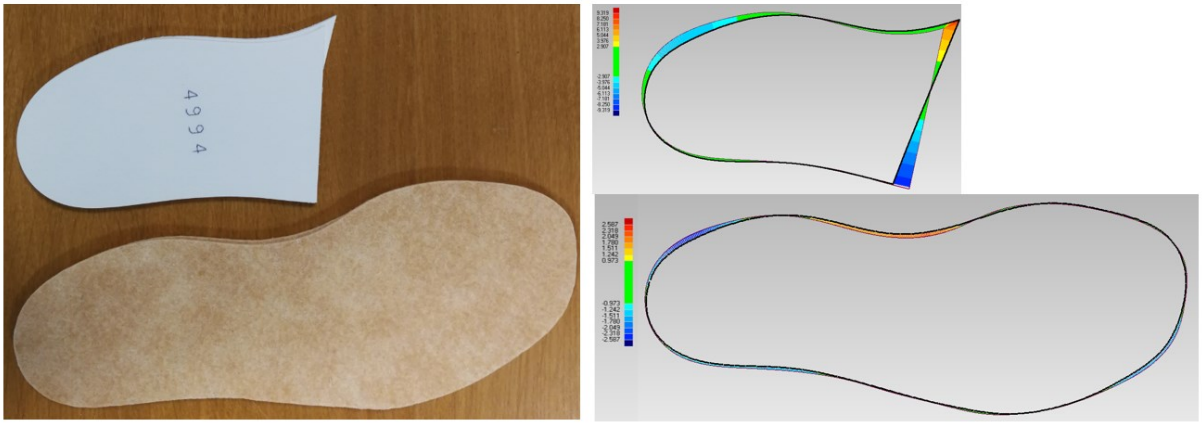


*Figure 6.3: Physical and Digital comparison of Footbed and Heel Reinforcement curve for subject 2 of Table 6.4. On the left is shown the physical comparison while on the right the digital one.*

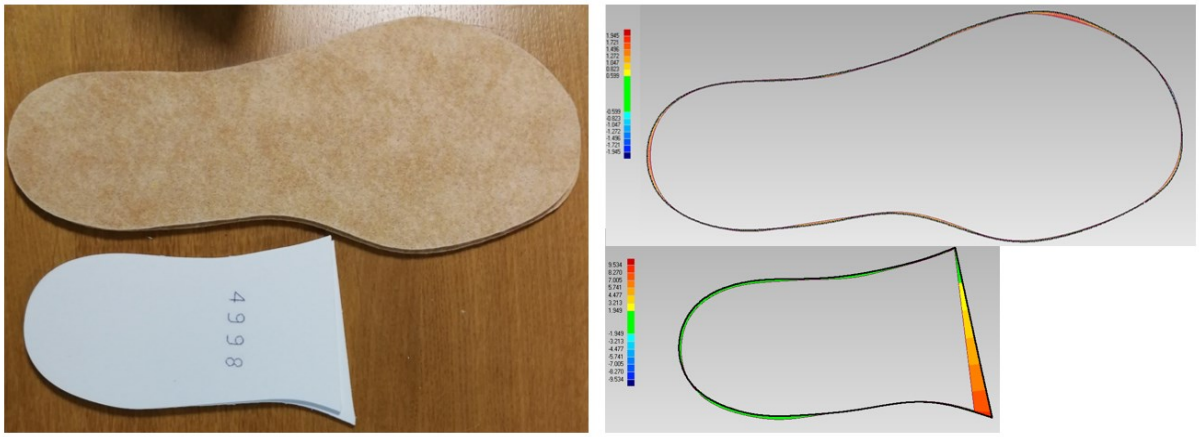


*Figure 6.4: Physical and Digital comparison of Footbed and Heel Reinforcement curve for subject 2 of Table 6.4. On the left is shown the physical comparison while on the right the digital one.*

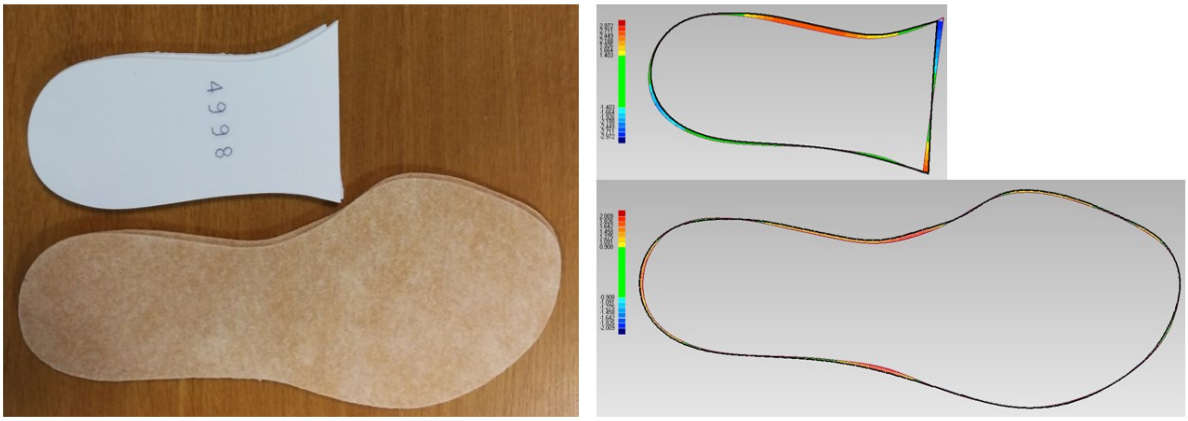


*Figure 6.5: Physical and Digital comparison of Footbed and Heel Reinforcement curve for subject 1 of Table 6.4. On the left is shown the physical comparison while on the right the digital one.*

The results obtained with the four additional lasts, used to perform both digital and physical comparisons, shown a digital comparison in accordance with the trend of the other 90 meshes analyzed. Moreover, the physical confrontation give the possibility to focalize the real impact of the error provided with the new procedure.

An example of a physical comparison with the last is reported in Figure 6.6. It shows the physical last with the corresponding footbed designed with the two different procedures. The two footbeds are placed in their position of application in order to evaluate the fitting with the last. The lower is the element designed with the new procedure while the upper one is the Duna S.r.l. footbed.

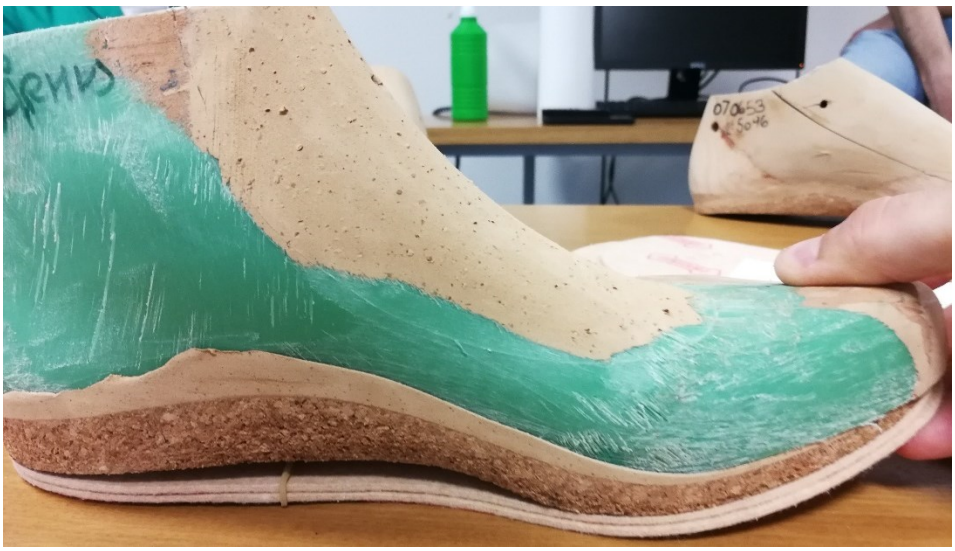

*Figure 6.6: Physical comparison with the last. The physical last with the corresponding footbeds. The upper one is the Duna S.r.l. element and the lower one is the new procedure element.*

In particular, it is possible to observe that in some points the difference between the two element is less significant that in the digital comparison. This is due to the fact that, based on the experience acquired over the time, the CAD technician draws the initial curve of the component slightly wider.

This strategy is purely related to the fact that a final element larger than necessary can be easily trimmed to obtain the correct size. On the contrary, a smaller component than required, will be discarded and will have to be redesigned.

Based on these considerations, an average deviation of about 1 mm for the footbed design can be considered tolerable given the strategy adopted by Duna S.r.l. CAD technician. However, for the heel reinforcement, the maximum acceptable angle deviation is about 3°, as higher values result in too high deviation.

From the analysis of the results it is possible to affirm that the new procedure has a good accuracy with regard to the design of the footbed and benefit sole, while it is less accurate in identifying the medial line that delimits the heel reinforcement in a limited number of lasts.

Therefore, the new procedure maintains the accuracy and precision required by the elements for custom-made footwear and, at the same time, reduces the design time compared to the procedure currently used by the company. In fact, the algorithm directly designs the curve on mathematically identified points avoiding the manual identification, adaptation and projection of the poly-curve by the CAD technician.

Moreover, the mathematical points extraction increases the repeatability and the robustness of the footbed design procedure, allowing also the least specialized and competent CAD technicians to design these components.

# 7 Conclusions

The custom-made orthopedic footwear is one of the most efficient non-surgical treatment in patients with severe pathologies or deformities. However, being built for the individual patient, it requires a high effort in design and production with a relatively high cost.

The strong computerization of the development process of this medical device, occurred in the last decades, aims to reduce the effort of design and realization of the various custom-made footwear components in favor of greater accuracy and efficiency, preserving also the aesthetic component of the shoe.

It is in this perspective that this thesis has been developed. In fact, the aim of this work was the development of an algorithm able to automatically extract the profile curves of footbed and other related components starting from a scan of last. This would reduce the design effort of the CAD technician in favor of a more accurate and repeatable procedure.

The goal has been achieved at least in part. In fact the new procedure has an automatic extraction of the points that characterize the profile curve and the medial curve necessary for the footbed and heel reinforcement design.

The results show that the curves designed with the new procedure have a good accuracy and are comparable to those designed by the technician of Duna S.r.l. for the Preprocessed dataset. Thus, the mesh preprocessing is essential to increase the quality of the final curves.

The fact that the feature points are mathematically computed by the algorithm, increases also the repeatability and the robustness of the design process.

However, even if the points that identify the lateral and medial profile have an easy recognizable conformation, the algorithm studies the curvature of the entire mesh and therefore it identifies not only the points of interest but also some points in excess. Thus, the excess points represent a first limitation of this new procedure.

Worse results have been obtained for the heel reinforcements. For these elements the main limitation is due to the low accuracy of the medial line identification. However, it concerns only some shapes analyzed and this could be related to the footwear model for which the algorithm finds difficulties in the analysis of the lower surface of the mesh, due to the low level of curvature.

In conclusion, the algorithm shows excellent results in identifying the lateral profile of the components, probably related to the fact that the lateral curvature of the digital last has a well identifiable trend. Instead, for what concern the identification of the medial line corresponding to the metatarsal joint, in some footwear model the error is greater than others, thus increasing the error also in the final design of the heel reinforcement .

Further studies could focus on improving the criterion of selection of characteristic points. In particular, it can be implemented an additional algorithm able to extract only the points that characterize the footbed profile and the medial line for the design of the heel reinforcement.

Moreover, a classification of the footwear model on which the algorithm work better could be performed in order to understand which are the footwear characteristics suitable for a good individuation of the medial line.

Finally, a Rhinoceros plug-in could be developed in order to include the entire procedure for extracting characteristic points and subsequent steps in a limited number of dedicated commands. The automation of this procedure will drastically reduce the design time of these elements by avoiding all the manual steps performed by the CAD technician. In this way the algorithm could be fully integrated into the production process of the company.

# 8 Bibliography


[1] K. Hildebrandt, K. Polthier, M. Wardetzky, *Smooth Feature Lines on Surface Meshes*, Proceedings of the third Eurographics Symposium on Geometry Processing, 136-141, 2005.

[2] F. Mattogno, G. Rosellini, E. Di Stanislao, G. Denza, *Calzature Ortopediche Su Misura,* Manuale Dispositivi Ortopedici ITOP S.p.A. Officine Ortopediche, 10-15, 2020.

[3] G. Milano, R. Betti, A. Becarelli, *Dizionario Inglese*, Garzanti il nuovo dizionario Hazon, 555 , 2000.

[4] Vircos, *Circonferenza caviglia*, Presamisure Vircos, 11, 2020

[5] P.W. Anggoro, B. Bawono, J.Jamari, M. Tauviqirrahman, A.P. Bayuseno, *Advanced design and manufacturing of custom orthotics insoles based on hybrid Taguchi-response surface method*, Heliyon , 7, 1-15, 2021.

[6] T.E: Sgarlato, *A compendium of Podiatric Biomechanics*, California College of Podiatric Medicine, 1971.

[7] M. Carroll, P. Molyneux, *Musculoskeletal Podiatric Medicine,* Neale's Disorders of the Foot and Ankle, 8, 160-221, 2020.

[8] H.F. Hlavac, *The Foot Book: Advice for Athletes*, World Publications, 1-385, 1977.

[9] K.T. Haendlmayer, N.J. Harris, *Flatfoot deformity: an overview*. Orthopedics and Trauma, 23, 395-403, 2009.

[10] J. Burns, J. Crosbie, R. Ouvrier, A. Hunt, *Effective orthotic therapy for the painful cavus foot: a randomized controlled trial*, Journal of the American Podiatric Medical Association, 96, 205-211, 2006.

[11] T. Buell, D. Green, J. Risser, *Measurement of the first metatarsophalangeal joint range of motion*, Journal of the American Podiatric Medical Association, 78, 439, 1988.

[12] J. F. Grady, T. M, Axe, E. J. Zager, L. A. Sheldon, *A retrospective analysis of 772 patients with hallux limitus*, Journal of the American Podiatric Medical Association, 92, 102-108, 2002.

[13] M. J. Coughlin, *Hallux valgus*, Journal of Bone and Joint Surgery, 78, 932-966, 1996.

[14] K. Rome, S. Stewart, *Rheumatic Diseases*, Neale's Disorders of the Foot and Ankle, 8, 222-260, 2020.

[15] L. Grondal, B. Tengstrand, B. Nordmark, P. Wretenberg, A. Stark, *The foot: still the most important reason for walking incapacity in rheumatoid arthritis: distribution of symptomatic joints in 1000 RA patients*, Acta Orthopaedica, 79, 257-261, 2008.

[16] J. Firth, C. Hale, P. Helliwell, J. Hill, E. A. Nelson, *The prevalence of foot ulceration in patients with rheumatoid arthritis*, Arthritis Care & Research, 59, 200-205, 2008.

[17] M. Edmonds, *Metabolic Disorders and Management of High-Risk Patients*, Neale's Disorders of the Foot and Ankle, 8, 261-281, 2020.

[18] D. G. Armstrong, A. J. M. Boulton, S. A. Bus, *Diabetic foot ulcers and their recurrence*, New England Journal of Medicine, 376 (24), 2367-2375, 2017.

[19] Duna S.r.l., *Technology and Services Catalogue*, Duna Innovation & Technology, 1-32, 2017.

[20] L. Fangyu, L. Yefei, W. Meiqiong, W. Jianfeng, *Research on Computer Aided Design of Customized Insoles*, Computer-Aided Industrial Design & Conceptual Design, 1430-1433, 2009.

[21] S. J. Lochner, J. P. Huisson, S. S. Bedi, *Parametric Design of Custom Foot Orthotic Model*, Computer-Aided Design & Applications, 1-11, 2012.

[22] M. Mandolini, M. C. Vitali, A. Macchione, R. Raffaeli, M. Germani, *A CAD Tool to Design Bespoke Insoles for Severe Orthopaedic Treatments*, Computer-Aided Design and Applications, 1-10, 2015.

[23] J. A. Bernabeu, M. Germani, M. Mandolini, M. Mengoni, C. Nester, S. Preece, R. Raffaeli, CAD tools for designing shoe lasts for people with diabetes, Computer Aided Design, 45 (6), 977-990, 2013.

[24] R. L. Actis, L. B. Ventura, D. J. Lott, K. E. Smith, P. K. Commean, M. K. Hastings, M. J. Mueller, *Multi-plug insole design to reduce peak plantar pressure on the diabetic foot during walking*, International Federation for Medical and Biological Engineering, 46, 363-371, 2008.

[25] Y. C. Hsu, Y. W. Gung, S. L. Shih, C. K. Feng, S. H. Wei, C. H. Yu, C. S. Chen, Using an Optimization Approach to Design an Insole for Lowering Plantar Fascia Stress – A Finite Element Study, Annals of Biomedical Engineering, 36 (8), 1345-1352, 2008.

[26] ParoCountour®-System, https://paromed.de/medien/medienpool/paroContour-System-4S-EN2.pdf, Paromed.

[27] Insole-Designer, https://www.pedcad-foot-technology.com/technical-equipment/software-solutions/design-software/ , Pedcad.

[28] Canfit™ Insole Design Software, https://vorum.com/insole-design/, Vorum.

[29] IcadPAN INESCOPE, https://www.inescop.es/en/services/software-for-footwear, INESCOP.

[30] Insole Designer, https://mecsoft.com/blog/rhinocam-does-custom-orthotics-in-italy/, Duna S.r.l.

[31] Duna S.r.l., *Sottopiedi Su Misura*, Duna Innovation & Technology, 2021.

[32] H. Liu, N. Dai, B. Zhong, T. Li, J. Wang, *Extract Feature Curves on Noisy Triangular Meshes*, Graphical Models, 93, 1-13, 2017.

[33] V. B. Sunil, S. S. Pande, *Automatic recognition of features from freeform surface CAD models*, 40 (7), 502-517, 2008.

[34] V. Vidal, C. Wolf, *Robust Feature Line Extraction on CAD triangular Meshes, Proceeding of the International Conference on Computer Graphics Theory and Applications*, 106-112, 2011.

[35] K. Demarsina, D. Vanderstraeten, T. Volodine, D. Roose, *Detection of closed sharp edges in point clouds using normal estimation graph theory*, Computer Aided Design, 39 (2), 276-283, 2007.

[36] T. Varady, A. F. Michael, Z. Terek, *Automatic extraction of surface structures in digital shape reconstruction*, Computer-Aided Design and Applications, 39 (5), 379-388, 2007.

[37] C. Mehdi-Souzani, J. Digne, N. Audfray, C. Lartigue, J. Morel, *Feature Extraction from High-density Point Clouds: Toward Automation of an Intelligent 3D Contactless Digitizing Strategy*, Computer-Aided Design and Applications, 7 (6), 863-874, 2010.

[38] M. Kolomenkin, I. Shimshoni, A. Tal, *Multi-Scale Curve Detection on Surfaces*, IEEE Conference on Computer Vision and Pattern Recognition, 225-232, 2013

[39] Y. Ohtake, A. Belyaev, H. P. Seidel, *Ridge-Valley Lines on Meshes via Implicit Surface Fitting*, ACM Transactions on Graphics, 23 (3), 609-612, 2004.

[40] S. Yoshizawa, A. Belyaev, H. P. Seidel, *Fast and Robust Detection of Crest Lines on Meshes*, Proceedings of the 2005 ACM symposium on Solid and physical modeling, 227-232, 2005.

[41] J. Huang, C. H. Menq, *Automatic Data Segmentation for Geometric Feature Extraction from Unorganized 3-D Coordinate Points*, IEEE Transactions on Robotics and Automation, 17 (3), 268-279, 2001.

[42] Y. An, Z. Li, S. Cheng, *Feature Extraction from 3D Point Cloud Data Based on Discrete Curves*, Mathematical Problems in Engineering, (4), 1-19, 2013.

[43] J. P. Thirion, *The Extremal mash and the understanding of 3d surfaces*, International Journal of Computer Vision, 19 (2), 115-128, 1996.